Preprint of Chapter 4 in the book "Aromaticity: Modern Computational Methods and Applications"
Ed. Israel Fernandez, Pub. Elsevier, May 2021

NICS – Nucleus Independent Chemical Shift

Renana Gershoni-Poranne and Amnon Stanger

"With great power comes great responsibility." – the Peter Parker principle, Spider-Man, Stan Lee

The Nucleus Independent Chemical Shift (NICS) method[1] was introduced by Paul v. R. Schleyer in 1996 as a computational tool for the evaluation of aromaticity, exemplified for monocyclic systems. Since then, the easy-to-use NICS technique has become the computational method of choice for identification and quantification of aromaticity.[2–4] However, the user-friendliness of NICS is a double-edged sword. On the one hand, it has made the study of aromaticity significantly more accessible to non-expert users and has contributed to a wealth of knowledge and insight into aromatic systems. On the other hand, it can mislead users into thinking that the interpretation of NICS results is as simple as running the calculation itself.

In this chapter, we provide a critical review of all things NICS. We describe the various versions of NICS methods that are available, including their differences and inherent limitations. We discuss common mistakes in using and interpreting NICS results and list "dos" and "don'ts" for more accurate chemical insight, depending on the information that is sought.

Historical and Physical Background of NICS

The NICS method is one of several that fall under the magnetic criteria of aromaticity,[3] meaning, it uses the response of an aromatic system to an external magnetic field to identify and quantify aromatic character. The shared physical basis for all of the magnetic criterion-based methods is commonly known as the Ring Current Model (RCM), which was developed separately by McWeeny[5] and Pople,[6] based on the Hückel-London formalism.[7,8] An interesting review of the history behind this model was written a few years ago by Dickens and Mallion.[9] In simple terms, the RCM compares a cyclically conjugated molecule to a circular wire, with the π electrons in this chemical system being analogous to the freely moving electrons in the metal wire. Just as electrons in a wire loop move in a circular fashion when the loop is placed in an external magnetic field, the RCM assumes that the cyclically delocalized electrons in the conjugated cyclic system also have circular motion. The circular (i.e., ring-like) motion of these electrons, is induced by the existence of the external magnetic field, and is therefore called an *induced ring current*. Following Ampere's circuit law and Maxwell's equations, as a result of the induced ring current, a new, *induced magnetic field* is generated, as well (Figure 1).

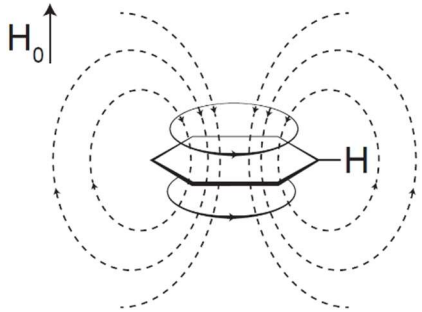

Figure 1. Depiction of the induced ring current and induced magnetic field in benzene. H_0 is the external magnetic field in the direction perpendicular to the molecular plane. For clarity, only one hydrogen atom is shown explicitly. The induced field in the

vicinity of the hydrogen has a deshielding effect, leading to the characteristic ^{1}H-NMR chemical shift of benzene. Reproduced from Reference 3 with permission from the Royal Chemical Society.

It is important to note that it is not only cyclically conjugated systems and their π-electrons that are affected by the external magnetic field; the same is true for all electrons in any given molecule. The difference stems from the fact that, in most cases, the electrons in localized bonds (e.g., σ-bonds and, to a lesser extent, isolated π-bonds) are tightly bound, and therefore do not move around freely. As a result, their induced currents, and in turn induced magnetic fields, are usually small. For cases where the electrons can move freely (i.e., delocalize), the resulting induced currents are significant and lead to large induced magnetic fields. Such is the case in aromatic and antiaromatic systems.

The overly simplified description afforded by the RCM may provide an intuitive understanding of why ring currents are formed. However, despite the development of more sophisticated RCM versions over the years,[10] it remains far from complete. For one thing, it treats all cyclically conjugated systems the same way, meaning it cannot differentiate between aromatic and antiaromatic systems. In contrast to the classical case of electrons in a wire loop, in the quantum case of a molecule, the electrons in cyclically conjugated systems can have circular motion in one of two directions: diatropic or paratropic. These terms come from the terms dia- and paramagnetic. Diamagnetic (paramagnetic) molecules are repelled (attracted) by a magnetic field, or an applied magnetic field causes them to generate an induced magnetic field that opposes (enhances) the external field. In monocyclic systems, for (4n + 2) numbers of π electrons, the induced current is termed diatropic because it leads to an induced field at the center of the ring that is anti-parallel (opposite) to the external field. This behavior changes outside the ring, however, where the induced magnetic field is in the same direction as the external field, and this deshielding causes the typical downfield shift of aromatic protons in ^{1}H-NMR spectra (Figure 1). For monocyclic systems containing 4n π electrons, the induced current is termed paratropic because it generates at the center of the ring a field that is parallel to the external field and opposes the external magnetic field outside the ring. The classically-derived RCM cannot explain how the change in π-electron count could afford opposing directions of electron motion.

The rationalization for these observations comes from analyses that demonstrate the relationship between orbital transitions caused by the external magnetic field and induced ring current values. Fowler and coworkers showed that, within the ipsocentric approach (also known as the continuous transformation of origin of current density-diamagnetic zero, CTOCD-DZ), the ring currents can be interpreted as stemming from the transition of electrons from occupied to unoccupied (i.e., virtual) orbitals.[11–13] Furthermore, because the strength of the contribution is proportional to the reciprocal of the energy of the transition (the difference in energy between the two orbitals participating in the transition), the aromatic (or antiaromatic) nature of a system is often dominated by the transitions of a small number of electrons in frontier molecular orbitals (MOs), for which this energy difference is smallest.[14] According to the analysis proposed by Fowler and coworkers, the contributions are determined by the angular and linear momenta of each transition. For planar aromatic systems, under a perpendicular magnetic field, the relevant operators are those for rotation around the field direction and two right-angle translations within the molecular plane. A transition will make a diatropic contribution to the current if the product of the symmetries of the two orbitals involved in the transition contains a match to one such translation. The contribution will be paratropic if the product of symmetries of the two orbitals contains a match to the rotation operator. A transition can be active with respect to either of these operators, both, or neither. Furthermore, the spatial distribution of the pair of orbitals will also determine the

magnitude of the contribution, i.e., they need to occupy the same region of space.[11,13,14] To demonstrate, let us study two examples: benzene and cyclooctatetraene. Figure 2a displays the doubly degenerate highest occupied MOs (HOMOs) and doubly degenerate lowest unoccupied MOs (LUMOs).

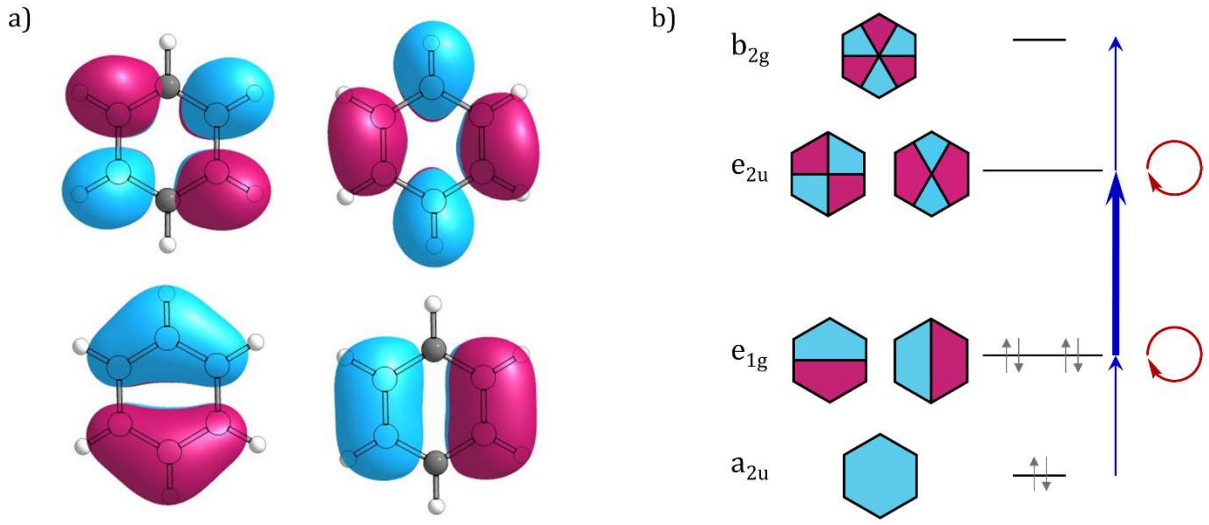

Figure 2. a) Frontier MOs of benzene. Top: degenerate LUMOs; Bottom: degenerate HOMOs. b) Fowler and Steiner's symmetry-based selection rules for rotational and translational transitions and their relationship to ring currents in benzene. Red arrows indicate rotational transitions and blue arrows indicate translational transitions. The wider arrow indicates the most contributing transition.

Note that the HOMOs have one node each, while the LUMOs have two nodes each. The rotation operator only mixes orbitals with the same number of nodes, i.e., it can relate the two HOMOs to one another and the two LUMOs to one another, but it does not allow mixing of the HOMOs and LUMOs. Thus, no paratropic contributions are generated. The translation operator mixes orbitals that differ by ±1 node, i.e., orbitals that are directly above/below each other on the energy diagram. The only occupied—virtual transitions that obey this constraint are the HOMO to LUMO transitions, and thus a diatropic contribution to the current will be generated. Figure 2c shows these transitions for benzene.

In contrast, the 4n π systems undergo a Jahn-Teller distortion. As a result, their HOMO and LUMO can be seen as a linear combination of the doubly degenerate SOMOs of the respective D_{nh}-symmetric system and therefore they have the same number of nodes (Figure 3 shows these orbitals for cyclooctatetraene). As stated above, the rotation operator allows mixing of orbitals with a similar number of nodes. This means that there will be an allowed rotational transition from HOMO to LUMO, leading to a paratropic contribution to the current. Moreover, because the HOMO-LUMO gap results from a Jahn-Teller effect, it is small. This is the reason that paratropic currents in antiaromatic systems are generally much stronger than diatropic currents in aromatic systems. In addition, there are no diatropic contributions, because there are no possible transitions between filled orbitals to virtual ones with one more node (i.e., transitions for which the product of symmetries would match the translation operator). Figure 3c shows these transitions for D_{4h} cyclooctatetraene.

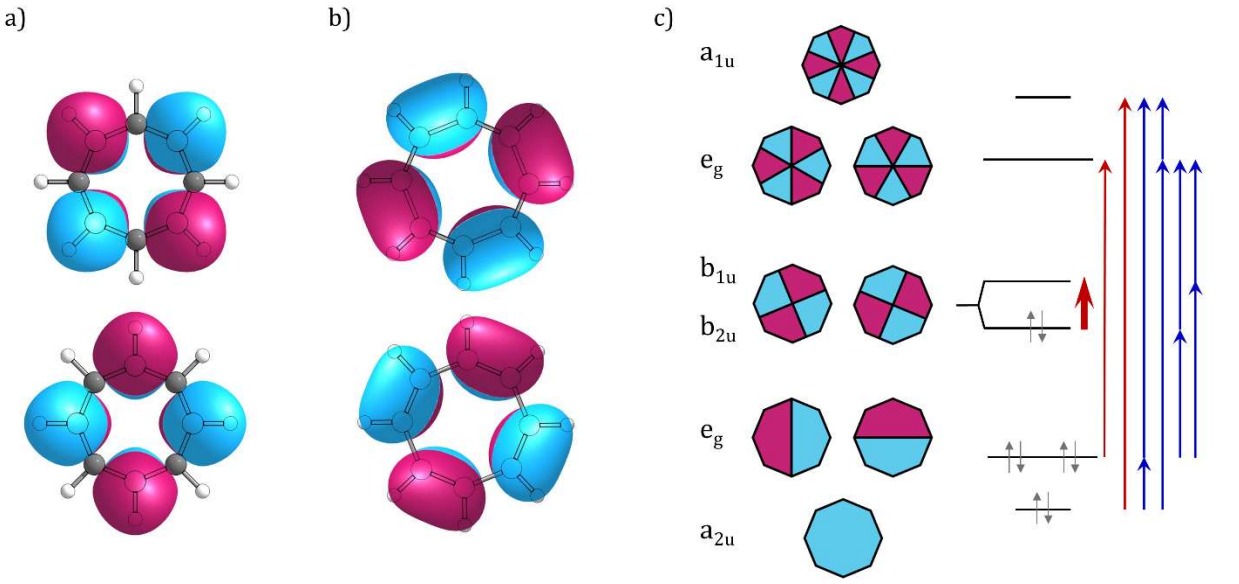

Figure 3. a) SOMOs of D8h triplet cyclooctatetraene. b) HOMO (bottom) and LUMO (top) of D4h cyclooctatetraene. c) Fowler and Steiner’s symmetry-based selection rules for rotational and translational transitions and their relationship to ring currents in D4h cyclooctatetraene. Red arrows indicate rotational transitions and blue arrows indicate translational transitions. The wider arrow indicates the most contributing transition.

Based on the approach demonstrated above, Fowler and coworkers proposed general definitions of orbital contributions for interpretation of properties of magnetizability and nuclear shielding, founded on symmetry, topology, and energy-based selection rules.

The relationship between rotational transitions and paratropic contributions to the current was later corroborated by Perez-Juste and coworkers within the gauge-including atomic orbital (GIAO) approach.[15] However, within GIAO, aromatic molecules are dominated by gauge transformations and specific links between orbital transitions and diatropic contributions cannot be identified. As mentioned above, our focus in this chapter is on the use and application of NICS-based methods. Therefore, beyond showing these main features, we will not detail here the mathematical formulations that connect NICS to these orbital contributions. However, we encourage readers interested in the formal derivations to refer to References 11-14.

The different methods housed underneath the magnetic criterion are all based on the underlying assumption that the strength of the induced ring current is related to the “amount” of aromaticity that a molecule has, and they propose various ways to quantify it. For example, Current Density Analysis (CDA),[12] Gauge-Including Magnetically Induced Currents (GIMIC),[16] and Anisotropy of the Induced Current Density (ACID)[17] are computational methods that directly study the induced ring current. Other methods focus not on the current itself, but on the properties that arise from it. For example, NMR chemical shifts of hydrogens and carbons in aromatic systems indicate the presence and strength of the induced magnetic field, and thus provide an indirect assessment of the current.[18] Yet, as Lazzeretti and coworkers warn, downfield protons are not reliable means for measuring aromaticity.[19] Similarly, bridgehead atoms, Li^+ ions, or endohedral ^{3}He atoms were previously used as experimental or computational probes for the induced magnetic field.[2] However, they suffer from severe drawbacks as well; chiefly, that they are not truly innocent bystanders, because their presence affects the chemical shift that it reported. Therefore,

while the concept of evaluating aromaticity through the strength of the induced magnetic field has merit, the practice of doing so is not straightforward.

NICS belongs to the latter category of methods. It is a computational tool that evaluates aromaticity indirectly, by reporting the chemical shift at a location in space, thereby indicating the strength of the induced magnetic field at that location. The NICS value is defined as the negative of the absolute shielding. Generally, NICS > 0 indicates a paratropic current, and NICS < 0 indicates a diatropic current. In the Gaussian suite of programs, the NICS probe is named "BQ" after the ghost *Banquo* in Shakespeare's Macbeth, so it is often referred to as a "ghost atom" in the literature. From a computational perspective, it is important to note that in Gaussian NICS probes are "dummy atoms" (which have no nucleus and no basis functions), not "ghost atoms" (which have zero nuclear charge, but serve as a center for basis functions). Though the concept is similar to the abovementioned probe atoms, the breakthrough is in the fact that NICS—as its name implies—has no nucleus. This is what allows it to act as an innocent observer—to report a chemical shift at a given location without influencing it by its mere presence at that location. Yet, from a user's perspective, it is treated just as one would place an atom at a certain location in space, which makes it incredibly easy to use. This idea, which we described as "ingenious in its simplicity" in a previous review,[3] is at the core of Schleyer's NICS method. Sadly, it is often overlooked (by us, as well) that it was, in fact, proposed prior to the original 1996 publication. As early as 1990, Fowler, Lazzeretti, and Zanasi performed an extrapolated *ab initio* calculation that predicted the chemical shielding within C_{60}.[20] In 1995, they verified the result with an explicit calculation and benchmarked it against the experimental value obtained by then.[21] Separately, Bühl and Wüllen reported in the same year on a computational evaluation of ring currents of various fullerenes by calculating endohedral chemical shifts—"by just computing the magnetic shielding of an appropriate point in space."[22] This is, in essence, what NICS does. Though the success of NICS is, without a doubt, due not only to the simplicity and elegance of its approach, but also to the insight Schleyer and coworkers derived from it and how they applied it to other aromatic systems, we believe it is important to credit the previous work, as well.

Evolution of NICS as an Aromaticity Index

Before we can discuss the evolution of NICS-based methods for the evaluation of aromaticity, it is important to issue a warning regarding the connection between NICS and aromaticity.

Firstly, we emphasize that aromaticity cannot be measured directly, nor can it be calculated from first principles. As is sometimes pointed out in the recurring debates about the validity of the concept of aromaticity itself, there is no "aromaticity component" in the Hamiltonian. In other words, none of the methods (including NICS) actually measures "aromaticity". Secondly, we note that, though NICS is predominantly used for the assessment of aromaticity, its formulation and application are entirely independent of the concept of aromaticity. In the simplest of terms, a NICS probe reports a chemical shift (the negative of the absolute magnetic shielding) at the location it is placed. NICS probes can be placed in the vicinity of any type of molecule and they will report a value. Whether these values indicate aromaticity or antiaromaticity, and if so, to what extent, is a matter of interpretation. The interpretation becomes even more complex when one considers that there is no fundamentally-derived relationship that connects the magnetic-criteria indices specified above to other measures of aromaticity (e.g., aromatic stabilization energy, ASE), nor is there a general empirical relationship. Therefore, one should remember that

whenever magnetic indices (such as NICS) are used for determination of aromaticity, they actually measure magnetic aromaticity.

Having said that, NICS is a very effective tool for identifying and quantifying magnetic aromaticity, when used correctly. The question then is, what does it mean to use it correctly? The first step is to understand the different versions of NICS and the limitations that accompany each one. Herein, we describe the chronological development of the different NICS versions. To make comparisons as clear as possible, we distinguish the different NICS versions according to the number of probes they use: those that use a single NICS probe and those that use several. Furthermore, we discuss the treatment of monocyclic systems separately from polycyclic systems.

NICS methods for Monocyclic Systems

Single-point NICS Methods

The classification "single-point NICS methods" refers to methods that use a single NICS probe to assign and quantify aromaticity. The methods differ in the location where the probe is placed and in the way the value is calculated, namely, what contributions are contained within the value. The methods included within this classification are denoted as follows:

1. $\mathrm{NICS}(0)$
2. $\mathrm{NICS}(1)$
3. $\mathrm{NICS}(\mathrm{r})_{\mathrm{ZZ}}$
4. $\mathrm{NICS}(\mathrm{r})_{\pi}$
   a. LMO-NICS
   b. CMO-NICS
   c. The σ-Only Model
5. $\mathrm{NICS}(\mathrm{r})_{\pi\mathrm{ZZ}}$

In the original version of NICS, introduced by Schleyer and coworkers in 1996,[1] the nucleus-independent probe was placed at the non-weighted (geometric) center of the ring under study. The rationalization for this choice was based on the expectation that the induced field would be maximal at this location, and the calculation would be most straightforward. This type of NICS measurement is nowadays referred to as $NICS(0)$, in order to specify that the height above the molecular plane is 0 Å. Figure 4 shows a pictorial depiction of the $\mathrm{NICS}(0)$ probe in benzene, as well as a Gaussian input file for calculating this metric. In the seminal 1996 work, the results of $\mathrm{NICS}(0)$ values for a series of five-membered heterocyclic systems showed a remarkable correlation with the respective ASEs. In contrast to ASE, however, NICS calculations did not require a non-aromatic reference system or calibration with homodesmotic equations. To conform to the conventions of NMR chemical shift measurements, the NICS values were reported with reversed signs: negative values denoted aromaticity and positive values denoted antiaromaticity. Schleyer and coworkers noted difficulty with treating three-membered ring systems, due to local shielding effects of nearby σ bonds, but claimed that these same effects were not significant in the larger ring systems. However, it quickly became apparent that nearby σ electrons do indeed generate induced currents (which are usually, but not always, paratropic), and that these may be of similar magnitude as the induced field generated by the π-electrons. These so-called "σ-contaminations" may mask the behavior of the π-system and lead to mistaken assignations of aromatic character.

a)

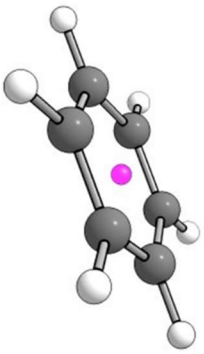

b)

```
# B3LYP/6-311+G**/AUTO NMR=GIAO INTEGRAL=(GRID=ULTRAFINE) CPHF=(GRID=FINE)

benzene

0 1
C        1.100160000      0.856040000      0.000000000
C       -0.191220000      1.380690000      0.000000000
C       -1.291380000      0.524720000      0.000000000
C       -1.100160000     -0.856040000      0.000000000
C        0.191220000     -1.380690000      0.000000000
C        1.291380000     -0.524720000      0.000000000
H        1.956030000      1.521980000      0.000000000
H       -0.340030000      2.454850000      0.000000000
H       -2.296000000      0.933030000     -0.000010000
H       -1.956030000     -1.521980000      0.000000000
H        0.340030000     -2.454850000      0.000000000
H        2.296000000     -0.933030000      0.000010000
Bq       0.000000000      0.000000000      0.000000000
```

Figure 4. a) Figure showing the placement of the NICS(0) probe in benzene. b) excerpt from a Gaussian input file, demonstrating the calculation of the NICS(0) metric for benzene.

The immediate solution was simple—to raise the NICS probe 1 Å above the molecular plane, affording the $NICS(1)$ value.[23] This height was later corroborated with a grid-based study, which mapped NICS values at various points around the ring.[24] Because the σ-effects decay rapidly with height but the π-effects do not, this means the σ-contaminations are significantly reduced. Indeed, for a time, it was considered that this solution effectively nullified the σ-contaminations altogether.

Both $\mathrm{NICS}(0)$ and $\mathrm{NICS}(1)$ are used analogously to measuring NMR chemical shift in solution. In other words, the value reported is the negative of the *isotropic* absolute shielding of the probe, which is the average value of the diagonal elements of the 3x3 shielding tensor. The tensor itself has 9 components, which are directional in space, and thus contains more information. Specifically, in the interest of assessing aromaticity, the component of interest is the one that describes the effects of the induced current generated in the π-system. If one assumes that the molecule is lying in the *XY* plane, then the induced π-currents are above and below this plane, and the resulting induced magnetic field is parallel to the *Z* axis in the center of the molecule (see Figure 1). Therefore, in 2000 Steiner and Fowler suggested that the only component that should be relevant is the *ZZ* component of the shielding tensor (also referred to as the *out-of-plane* component).[25,26] Following the existing naming convention, this metric is known as $NICS(r)_{ZZ}$, where *r* is the distance of the probe from the molecular plane. Though this metric is more indicative than isotropic NICS metrics, one should keep in mind that σ-electrons can also generate currents in the *XY* plane, thus affecting the $\mathrm{NICS}(r)_{\mathrm{ZZ}}$ value. In other words, the calculated value does not necessarily originate from just the π-electrons, and thus does not necessarily reflect aromatic behavior. Moreover, even though taking only the *ZZ* component reduces the inherent σ-contaminations, it is still not recommended to place the probe within or close to the molecular plane.

Despite making significant improvement, neither $\mathrm{NICS}(1)$ nor $\mathrm{NICS}(r)_{\mathrm{ZZ}}$ solve the problem of contaminations stemming from σ-electrons. Furthermore, since the σ-contaminations within different systems vary with the height above the molecular plane (e.g., 1 Å), even a relative aromaticity scale may be problematic to obtain. Because it is only the π-electron currents that are related to aromaticity, these contaminations inhibit both a qualitative and a quantitative evaluation of aromaticity. A procedure to separate the contributions of the σ- and π-electrons to the chemical shielding would allow one to obtain a NICS value generated only by the π-electron currents, termed $NICS(r)_{\pi}$, which would be a more

accurate description of the aromatic behavior. This procedure, sometimes referred to as *dissection*, can be achieved with several approaches, which we detail below.

In the original version of $\mathrm{NICS}(r)_{\pi}$, called *LMO-NICS* (localized molecular orbitals-NICS), the Individual Gauge for Localized Orbitals (IGLO) method was used together with the Pipek-Mezey localization procedure to provide the contributions of individual LMOs to the chemical shift.[24] A correlation between $\mathrm{NICS(r)}_{\pi}$ obtained this way and other aromaticity indices (ASE and magnetic exaltation) was shown. At the time of writing this chapter, this method is rarely used, perhaps due to the computational expertise required and to the fact that it is not included in the computational software packages used by most organic chemists.

A second type of dissection procedure, known as *CMO-NICS* (canonical molecular orbitals-NICS) calculates the contribution of each CMO to the chemical shift within the Gauge-Including Atomic Orbital (GIAO) method.[27–29] GIAO performs the transformation under external magnetic field already at the atomic orbital level, prior to computing the MOs, which is why the contribution of each CMO to the chemical shielding is obtained and not the contribution of each MO. The resulting values are termed in this chapter $\mathrm{NICS}_{\pi}^{\mathrm{CMO}}$. It is a more reliable method, as the results are independent of gauge (origin) choice. Currently, the commonly-used implementation of this procedure employs the Natural Chemical Shielding (NCS)[30] method found in the NBO[31] programs, which interface with programs such as Gaussian[32] and ORCA.[33,34] This makes it rather easy to use, which perhaps contributes to its popularity.

The most refined version of NICS combines both of the modifications described above: taking *only* contribution of the π electrons and *only* the *ZZ* component of the chemical shielding tensor. This affords the metric termed $NICS(r)_{\pi ZZ}$. This can be achieved with the two dissection procedures mentioned above (LMO and CMO). Yet, it should be noted that they suffer from an inherent disadvantage: they make use of mathematical treatments to separate σ- and π-orbitals, which means they are useful for systems in which these orbitals can be easily separated—i.e., planar systems. Though a large number of aromatic systems are planar, there is also an enormous number of curved aromatic systems, to which these methods cannot be applied readily. Attempts have been made to introduce different practices for curved systems, such as taking NICS values 1 Å from the convex and the concave faces,[35] but these have not been widely adopted. An additional disadvantage is the fact that these methods make use of certain approximations (e.g., localization) and do not provide error estimations. A third dissection method, known as the *σ-Only Model*,[36] was introduced in 2010 and offers a different approach. In this model, one first calculates the $\mathrm{NICS}(r)_{\mathrm{zz}}$ value of a system of interest, e.g., benzene, by placing the NICS probe above the molecular plane. Then, one constructs an artificial system, whereby the geometry of the studied system is frozen, and hydrogens are added on the opposite face from the NICS probe, at a fixed distance (approximately 1 Å) from each of the centers participating in the π-system (Figure 5).

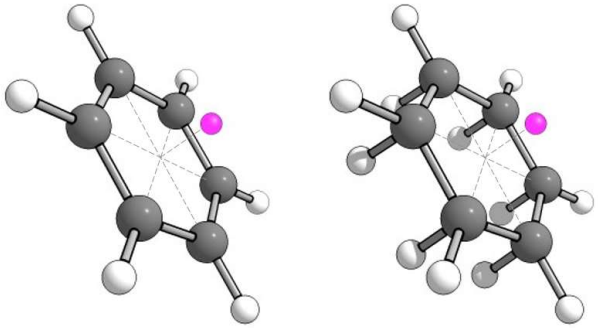

Figure 5. Left: Benzene with a NICS probe at a height of 1 Å above the molecular plane. Right: σ-Only model for benzene.

In the benzene example (Figure 5), this means a hydrogen atom below each of the six carbons. The idea is that these additional hydrogens form new C-H bonds, using the electrons in the p-orbitals. As a result, there are no C-C π-bonds and no delocalized π-electrons, hence the name "σ-Only". The user then calculates the $\mathrm{NICS(r)_{ZZ}}$ values for the "hydrogenated" system, which has no π-currents, and subtracts this value from the value of the delocalized system. The result reflects the clean π-contribution to the $\mathrm{NICS(r)_{ZZ}}$ value, i.e.,

$$(1) \qquad NICS(r)_{\pi ZZ}^{SOM} = \Delta NICS_{ZZ} = NICS(r)_{\mathrm{ZZ}}^{Del} - NICS(r)_{ZZ}^{Model}$$

Where $NICS(r)_{\pi ZZ}^{SOM}$ is the term we assign to $NICS(r)_{\pi ZZ}$ obtained with the σ-Only Model, $NICS(r)_{\mathrm{ZZ}}^{Del}$ is the NICS value of the delocalized system (the molecule under study) and $NICS(r)_{ZZ}^{Model}$ is the NICS value of the model system, in which hydrogens have been added.

One main advantage of this procedure is the fact that it can deal with non-planar systems. The second advantage is that it contains a built-in measure of accuracy. For a perfect model,

$$(2) \qquad NICS(r)_{\pi ZZ} = 3\Delta_{iso}$$

i.e., the difference between the delocalized and model systems is equal to exactly three times the difference in isotropic shielding. In practice, the difference between these two values is an indication for how accurate the calculation actually is. We note that this chemical model is mostly used in conjunction with the NICS-Scan method (see below, section on Multi-point NICS Methods).

Comparisons of the different versions of NICS to other metrics for aromaticity evaluation show that the more refined versions, $\mathrm{NICS}(r)_{\mathrm{\pi ZZ}}$ and $\mathrm{NICS(1)_{ZZ}}$, are generally more accurate for the investigation of aromaticity.[37,38] This means that the qualitative and quantitative conclusions drawn from these more refined methods have a closer agreement with other aromaticity criteria. This is not surprising, as they extract the salient contributions from the chemical shielding information.

To illustrate this point, consider the different NICS values obtained for some aromatic and antiaromatic systems using the various methods presented in Table 1. There is a wide variation in both the range of values obtained with the different NICS metrics, and the order of aromaticity that can be understood from these values. This highlights the importance of only comparing NICS values obtained with the same method, and the care that must be taken when making chemical conclusions based on this data.

Table 1. Comparison of various NICS values for some typical aromatic and antiaromatic compounds: benzene, pyrrole, furan, thiophene, D_{2h} cyclobutadiene, D_{4h} cyclooctatetraene.[a,b] All values reported in ppm.

$NICS(0)$	-8.0	-13.6	-11.9	-12.6	26.2	40.6
$NICS(0)_{zz}$	-14.5	-12.4	-8.8	-9.1	109.5	126.6
$NICS(0)_{\pi zz}^{CMO}$	-35.8	-32.1	-27.0	-27.0	55.9	112.7
$NICS(0)_{\pi zz}^{SOM}$	-38.4	-28.9	-24.9	-24.9	49.0	115.0
$NICS(1)$	-10.2	-10.1	-9.4	-10.2	17.3	32.1
$NICS(1)_{zz}$	-29.3	-31.0	-27.2	-28.0	55.0	97.2
$NICS(1)_{\pi zz}^{CMO}$	-29.1	-25.0	-20.3	-22.1	50.1	93.6
$NICS(1)_{\pi zz}^{SOM}$	-31.3	-22.4	-17.9	-19.4	45.9	94.6

[a] *All NICS values calculated at the B3LYP/6-311+G** level of approximation.*

[b] *All geometries optimized at the B3LYP/6-311G** level of approximation, except for cyclooctatetraene, which was constrained to planarity.*

The differences are easier to appreciate when displayed pictorially, as in Figure 6. The bar-plot depiction illustrates how the isotropic versions (at both 0 and 1 Å heights) have a condensed range of values, due to the masking effect of σ-contaminations. As a result, they minimize the differences between the molecules. Extracting only the *ZZ* component does not make much of a difference at the height of the molecular plane (which is not surprising), but shows a significant effect at a height of 1 Å, where the spatial extent of the π-system is much larger. The range of values does not change significantly when only the contribution of the π-electrons is considered, however, subtle differences appear. Namely, the order of aromaticity changes. For the collection of molecules shown here, the effect is more pronounced with $NICS(1)_{\pi zz}^{SOM}$ than with $NICS(1)_{\pi z}^{CMO}$, but there is no general rule that can be inferred from this. Overall, the two methods of dissection agree very well.

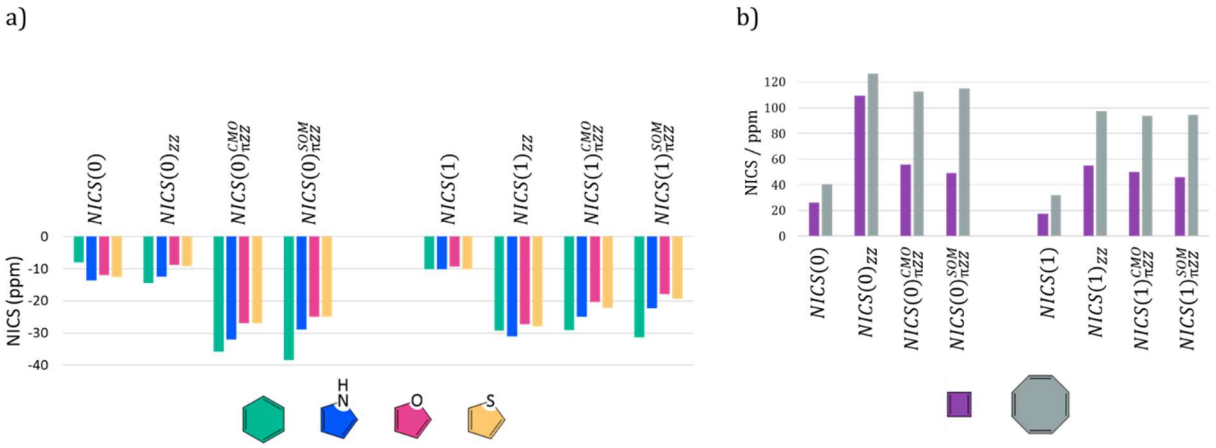

Figure 6. Bar plots of the various single-point NICS values of some representative a) aromatic and b) antiaromatic systems.

Despite the intrinsic limitations of less refined versions, over the years, all of the various NICS metrics have been used with varying degrees of success to study the aromatic character of a large and diverse collection of compounds, as well as to gain insight into mechanisms and transition states. At the same time, even the most refined versions may provide misleading results, and in some cases contradict conclusions based on other aromaticity indices. Some of these issues are related to inherent limitations of NICS, and thus cannot be solved within the realm of NICS-based methods. The most significant drawback and criticism of NICS, in all of its versions, is that it reduces the wealth of information contained in the vector field of the current density to a single scalar number. As Bultinck and coworkers recently showed,[39] this leads to a lack of uniqueness. Thus, though this reduction is what makes NICS such an easy tool to use, the same loss of information and nuance can lead not only to quantitatively wrong results, but even to qualitatively wrong chemical conclusions. One example is the case of cyclopentadiene, which was thought to have hyperconjugative aromaticity,[40] but was later shown to be non-aromatic.[41] Other problems, for example the over-interpretation of NICS values, can be solved by choosing the correct NICS metric (see last section in this chapter) and by using multidimensional NICS-based approaches, as we describe in the next section.

Multi-point NICS Methods

The term "multi-point NICS methods" encompasses all NICS-based methods that make use of more than one NICS probe. These can be generally classified into 1D and 3D methods. The former use NICS probes along a line, the latter use NICS probes in a grid formation (in some cases 3D grids are dissected into layers of 2D grids at different heights from the molecule). Multi-point NICS-based methods were developed to mitigate the loss of information inherent in using a single-point scalar value to describe the aromaticity of a system. As stated above, even the most refined version of NICS suffers from this drawback and, therefore, cannot provide a complete and nuanced description of the tropicity, and hence magnetic aromaticity, of a system. In the mildest case, this can lead to quantitatively misleading results. However, in the most extreme cases, it can lead to completely incorrect characterizations of compounds as aromatic/antiaromatic or non-aromatic, as we pointed out previously in our 2015 review[3] and as was demonstrated in the aptly titled "Not All That Has a Negative NICS is Aromatic" paper by Solà, Merino, and coworkers.[42]

The first example in the literature using multiple probes is not, strictly speaking, a NICS-based method. In 1999, Juselius and Sundholm introduced Aromatic Ring Current Shieldings (ARCS),[43] a method that uses magnetic shieldings calculated at discrete points along a line perpendicular to the molecular plane, starting at the center of the molecule. In ARCS, the computed shielding values are used to calculate the strength of the induced ring currents, using classical electrodynamics. The main advantages are the ability to compare systems of varying sizes and the cancellation of dependence on the strength of the applied field. The authors also demonstrated that non-aromatic systems exhibit qualitatively different profiles, which allows for correct characterization. Though ARCS has been used to evaluate aromaticity in a few cases,[44] to the best of our knowledge, despite the sound physical basis of this approach, it has not become a commonly-used tool, perhaps because it is not easily accessible (e.g., a standalone program is not provided, nor is it implemented in popular software programs). Nevertheless, it is important to note this seminal contribution, which demonstrated a novel approach to ameliorate significant problems with single-point NICS methods.

In 2001, Klod and Kleinpeter reported on the first use of NICS probes in a grid of lattice points around a molecule of interest.[45,46] The resulting values were plotted as isochemical shielding surfaces, which were used to study the influence of magnetic anisotropy. The original 2001 paper discusses quantitative conclusions that can be reached from comparison of different substituents (e.g., triple bonds and phenyl groups) in this way. However, for the purpose of evaluating aromaticity, this method is inappropriate, as it uses isotropic NICS values (see above for limitations of isotropic NICS indices). Secondly, though the pictorial depiction is good for intuitive understanding of magnetic behavior, it remains challenging to compare between different systems.

In the same year, Schleyer and coworkers used a similar grid-based approach to study benzene and cyclobutadiene.[24] In contrast to Klod and Kleinpeter’s work, this analysis used the LMO-NICS procedure to obtain $\mathrm{NICS}(r)_{\pi}$ values, which are more appropriate for the study of aromaticity. In their analysis, they studied not only the NICS values stemming from the π-orbitals, but also the values stemming from what they termed “core” orbitals. The dissection, in combination with the grid placement of probes, showed the respective contributions of core- and π-electrons at different location in and around the rings. This demonstrated very clearly how the total NICS value is influenced by σ-electrons when placed closer to the molecular plane and/or the bonds. In addition, the results showed the expected anisotropy cone and how the magnetic field changes its direction outside the ring (the latter effect is important in polycyclic systems). In contradiction to the previous case, which was proposed by Klod and Kleinpeter as a method for characterization of aromatic molecules, the Schleyer analysis was performed to compare the validity of the $\mathrm{NICS}(1)$, $\mathrm{NICS}(1)_{\pi}$, and $\mathrm{NICS}(0)$ indices, and was not suggested as a general approach for characterization of aromatic species. Combined with the high computational cost of calculating dissected NICS at such a large number of points, this may explain why this method is not widely used.

In 2006, Stanger proposed the *NICS-Scan*.[47] Similarly to ARCS, the 1D NICS-Scan method uses a series of probes placed along a line perpendicular to the molecular plane (Figure 7c), starting at the ring center—the line of the strongest induced magnetic field. Contrary to ARCS, however, the analysis itself remains at the level of NICS values (rather than calculating the current density), which makes it much simpler and faster to use.

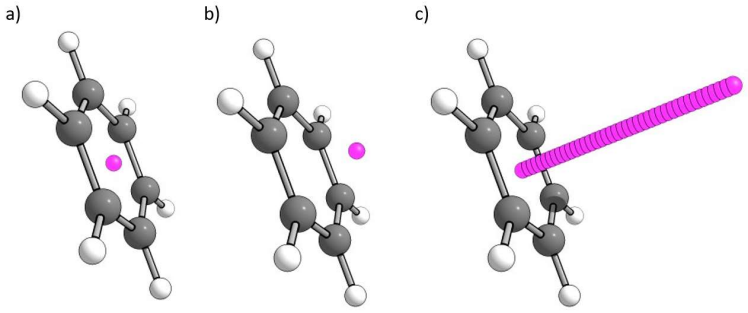

Figure 7. Comparison of different NICS probe placements for benzene: a) NICS(0); b) NICS(1); c) a NICS-Scan (series of NICS probes along a line perpendicular to the geometric center of the molecule, spaced at 0.1 Å intervals).

In principle, the NICS-Scan can be employed with isotropic NICS, but this would limit the interpretability in terms of magnetic aromaticity. Rather, common practice is to separate the individual NICS values into the *in-plane* and *out-of-plane* components, where out-of-plane is analogous to the *ZZ* component described above (when the molecule is in the *XY* plane). When these components are plotted against the

distance from the molecular plane, distinctive shapes are obtained for diatropic and paratropic systems, respectively. Typically, diatropic systems begin with a negative value that decreases until it reaches a minimum (usually at 0.8—1.2 Å above the molecular plane) and then decays slowly to zero at large distances. Paratropic systems begin with highly positive values that steadily decrease as the distance from the molecular plane is increased, decaying to zero at large distances. Figure 8 shows the NICS-Scans of benzene and cyclooctatetraene. As with ARCS, the emergence of characteristic shapes, in and of itself, already provides a more informative picture than singular NICS values do. This is especially useful in cases where the values are relatively small (close to zero) and a single value may not give an unambiguous interpretation. In such cases, the shape of the curve can help make a more informed judgement as to the nature of the system.

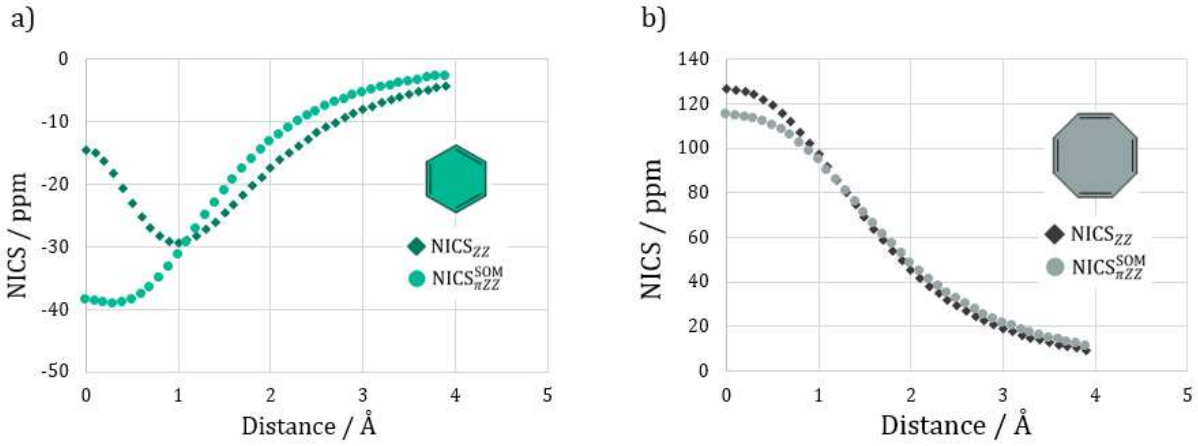

Figure 8. NICS-Scans with NICS$_{ZZ}$ and NICS$_{\pi ZZ}$ obtained with the σ-Only Model for a) benzene and b) D_{4h} cyclooctatetraene.

Furthermore, the depth and location of the minimum (in diatropic systems) or the maximal value (in paratropic systems) and the rate of decay can be useful for semi-quantitative comparison between different systems. To enable quantitative analysis of aromatic character, $\mathrm{NICS}(r)_{\pi Z}$ values must be used. These can be obtained using any of the dissection methods described above. Several studies have been published that use the NICS-Scan in conjunction with CMO-NICS and/or the σ-Only Model. For example, our own analysis of [N]phenylene isomers[48] uses the former, while our analysis of semiconductor oligomers uses the latter.[49] In addition, it is common to perform a fitting (logarithmic or polynomial have both been reported) of the values. For the fitting procedure, the points in the range $0 < r < 1$ Å are omitted, as these are most susceptible to contaminations from additional effects. Then, a function is fit to the data points in the range $1.1 < r < 3.9$ Å (for a scan done according to the default procedure in the range [0,3.9]) and the value for $r = 1$ Å is extrapolated from the fit. The rationale behind the fitting procedure is that by considering the points along the scan pathway that most cleanly describe the effect of the π-electrons, a better description of the induced magnetic field is obtained, and local effects or numerical inaccuracies are minimized.

Following a long period of inactivity in the development of NICS-based methods, in 2019 Stanger introduced a new approach, termed $\int NICS$.[50] Critics of NICS often note the dependence of $\mathrm{NICS}(r)_{\pi ZZ}$ values on the height r as a problem. Table 1 above demonstrates very clearly that NICS values change significantly with the location of the probe. The difficulty this causes is exemplified in the comparison of the three systems: benzene (**1**), cyclopentadienyl anion (**2**), and cycloheptatrienyl (tropylium) cation (**3**).

Depending on the value of *r*, the $\mathrm{NICS}(r)_{\pi ZZ}$ values lead to different orders of diatropicity. Namely, at *r* = 0 Å, the order of aromaticity is determined to be **2** > **1** > **3**; at *r* = 1 Å, the order of aromaticity is **1** > **2** > **3**; at *r* = 2 Å, the order of aromaticity is **3** > **1** > **2** (Figure 9).

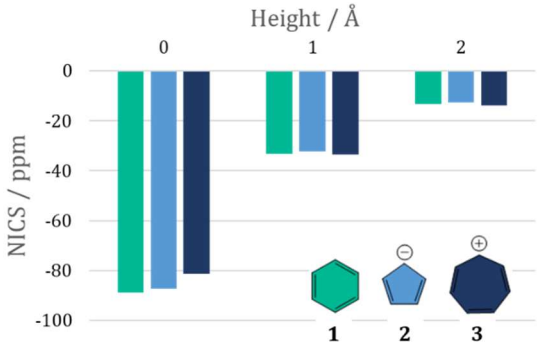

Figure 9. $NICS_{\pi ZZ}$ values for benzene, cyclopentadienyl anion, and cycloheptatrieny (tropylium) cation at heights of 0, 1, and 2 Å from the molecular plane. Values taken from reference[50] [505050].

The different orders are due to the different shapes and rates of decay of the ring currents in different systems. Because the cross-section of the ring current has a different radius for every molecule, a NICS probe at an arbitrary height only samples the induced magnetic field arising from the current around that height, and the maximal values will be at different heights for different molecules. Stanger argued that since the aromaticity of a molecule is related to the ring current in its entirety, in order to correctly describe the aromaticity, one must consider the ring current in its entirety. To do so, he proposed to use the total induced magnetic field, not just the value sampled at an arbitrary height, by integrating over all $\mathrm{NICS(r)}_{\pi ZZ}$ values along a 1D NICS-Scan.[50] Moreover, to obtain accurate values of the magnetic field induced by the clean π-ring currents, Stanger calculated the $\mathrm{NICS(r)}_{\pi ZZ}$ values in the range 2.0 < *r* < 5.0 Å, as this is the area where the induced magnetic field that is formed only from delocalized π-electrons is found. He then extrapolated the obtained the values in the region 0.0 < *r* < 2.0 Å and 5.0 < *r*. The values of $\int_0^\infty NICS(r)_{\pi ZZ}dr$ calculated for 13 systems show a good correlation with the respective $\mathrm{NICS(1)}_{\pi ZZ}$, but have the added benefit of circumventing the need to choose an arbitrary height for positioning the NICS probe. It can also provide an unambiguous answer to the order of aromaticity in cases such as the one presented above: $\int \mathrm{NICS}$ shows that tropylium (**3**) is the "most aromatic" of the three (although all three are very close). This method is very recent, and therefore it remains to be seen whether, over time, it will become a popular NICS-based method. Its usefulness will depend, as with the other metrics, on applying it to various systems and obtaining a database of values which enable comparison across various systems.

Looking back at the evolution of NICS metrics for monocyclic systems, we see that the initial years following the introduction of NICS (1996-2001) were marked by a flurry of activity, which led to the refinement of the metric to one with a sounder physical basis, which is appropriate for investigation of aromaticity. In this time, the place of NICS as a useful and easy tool for assessing aromaticity was solidified. The next major advancement was the transition to multidimensional methods. Following that, the field remained quiet for the most part. To our knowledge, Stanger's $\int \mathrm{NICS}$ metric was the first proposed modification in approximately a decade.

During this time, with the advent of new criteria and methods for evaluating aromaticity, a great deal of research has focused on the agreement of NICS with other aromaticity indices. From reading the literature, one gets the impression that there are two main types of NICS-users: casual users and expert users. Among the casual users, the use of $\mathrm{NICS}(0)$ and other older versions is still common, despite their shortcomings and the repeated attempts of many to warn against such practices. Within the expert users (mainly, the aromaticity community), there are two main camps: those who use NICS and advocate for safe and responsible interpretation and those who are deeply critical of NICS, usually due to its inherent limitations, and advocate for alternative methods. For those expert users who do employ NICS-based methods, the combination of the NICS-Scan with dissection procedures is considered to be the state-of-the-art and is used extensively. This is not to say that all criticisms of NICS have been answered. Rather, it appears to reflect more on the persistence of entrenched practices (for casual users) and on an acceptance of the inherent limitations of NICS (for expert users).

NICS methods for Polycyclic Systems

Analogously to calculating NICS above individual monocyclic systems, in the early 2000s it became common practice to calculate NICS above the individual rings of a polycyclic system. To date, this is still a common way of characterizing polycyclic systems, and in many cases, these values can be invaluable in mapping the magnetic behavior of such systems. The individual values are also sometimes summed to afford a global value. We have also used this approach on more than one occasion. For example, in 2012, we used such an approach to show concurrence between NICS and other indices of aromaticity,[48] in 2013 the charge-separation energy and aromaticity in fulvalene were correlated,[51] and in 2018 we used it to show relationships between the aromaticity of aromatic oligomers and their electronic properties (HOMO-LUMO gap and Ionization Potential).[49] The Mills group has also used this approach in their investigation of antiaromatic species.[52] In 2020, Alvarez-Ramirez and Ruiz-Morales published a database of isotropic NICS and $\mathrm{NICS_{ZZ}}$ values for 660 benzenoid polycyclic aromatic hydrocarbons (Figure 10),[53] which again highlights that this kind of information is important for characterization.

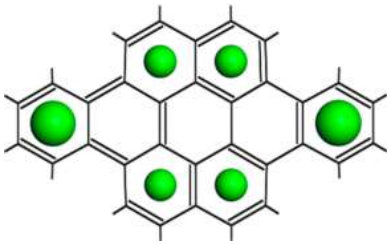

Figure 10. Example of the visualization of NICS values in the NICS database of Alvarez-Ramirez and Ruiz-Morales. The sizes of the green circles illustrate the relative magnitudes of the NICS values in the respective rings. Image reprinted with permission from Reference [53]. Copyright 2019 American Chemical Society.

Yet, as with all NICS-based methods, caution must be practiced. Quantification of aromaticity in polycyclic systems poses a unique challenge for NICS-based methods. This is because NICS—no matter how refined—cannot distinguish the origin of the induced magnetic field. In other words, it cannot differentiate between various currents co-existing in the same system, which is exactly the situation in polycyclic systems. These types of systems can simultaneously sustain local (one ring), semi-global (two or more rings), and global (encompassing the entire system) ring currents. In addition, even if ring currents are localized—e.g., as in the [N]phenylenes[48]—as mentioned above, each ring current creates an induced field outside the circumference of the ring, in the opposite direction. This was demonstrated very clearly

by Schleyer and coworkers in their grid-formation of NICS probes (Figure 11).[24] As seen in the image, the effect of each ring current can be seen outside the circumference of the molecular ring. This implies that in fused-ring systems, the value calculated above a given ring will contain contributions from the neighboring ring.

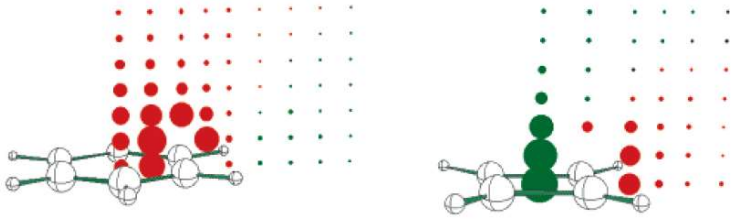

Figure 11. Visualization of the dissected NICS values in benzene (left) and cyclobutadiene (right). The size of the spheres corresponds to the magnitude of the NICS values and the colors correspond to their sign: green indicates positive values (paratropic), red indicates negative values (diatropic). Image reprinted with permission from Reference 24. Copyright 2006 American Chemical Society.

In other words, neighboring rings create small effects on each other. Thus, a NICS value above the center of one ring contains multiple different contributions and cannot be used to quantify the ring current within that specific ring, as was demonstrated by Bultinck and coworkers.[54] Interpreting the NICS values in this way can lead to problematic conclusions, such as the case of the "anthracene paradox".[55] In anthracene, the NICS values above the center ring are about 33% larger (in absolute value) than the neighboring rings, which would suggest a stronger aromatic character, according to the conventional interpretation of NICS. Yet, this center ring is also more reactive, for example in hydrogenation or Diels-Alder reactions, which would suggest it is less aromatic, according to the energetic criterion of aromaticity, if we consider each ring to be separate from the others. This apparent contradiction was solved by Bultinck and coworkers,[56] who proposed that anthracene sustains 6 different currents: 3 benzenic, 2 naphthalenic, and 1 anthracenic current. The center ring participates in the largest number of circuits and therefore has an increased current density around it, which is reflected in the NICS value. It does not, however, mean that this ring is individually "more aromatic" than its neighbors. GIMIC results support a slightly different interpretation, whereby anthracene sustains one global current encompassing all three rings, and in addition a local benzenic current in the central ring.[57]

This begs the more fundamental question: can we even speak in terms of "local aromaticity"? The term is pervasive in the literature,[58–61] yet we argue that the term "local aromaticity" in *cata*- and *peri*-condensed systems is misleading and that we should not consider individual rings within a fused polycyclic system as separate entities. Aromaticity is a molecular property—the π system is delocalized over the entire system and cannot be arbitrarily separated. Consider, also, that aromaticity indices such as ASE, resonance energy (RE), and diamagnetic exaltation susceptibility are defined for a system in its entirety.

On the other hand, we recognize that several methods specifically make use of such arbitrary decomposition to characterize the aromaticity of larger systems. Methods based, for example, on localization of electrons or additivity of subunits do this inherently. In our view, these methods can be very useful for characterizing and even predicting the aromatic behavior of whole system. Moreover, it is recognized that there are *local trends* in the aromatic behavior of polycyclic systems, i.e., certain parts of a molecule may contain weaker or stronger currents. It is also possible that one part of a fused polycyclic system will contain a paratropic current and another part will contain a diatropic current, and there are

even cases where one type of current exists within a larger circuit of the opposite type. Thus, the problem is not with the decomposition of polycyclic systems for analysis, per se, but with the interpretation of such results without the broader context, and we believe this is perpetuated by the term “local aromaticity”. To circumvent this, we propose the safer terminology of “local trends in aromatic character”—which allows discussion of different areas within a polycyclic aromatic system without making sweeping generalizations regarding the properties of the molecule as a whole. It is useful to know and understand these patterns.

Extending the rationale of the NICS-Scan, in 2014 we developed the NICS-*XY*-Scan.[62] Similarly to the NICS-Scan, this method uses a series of NICS probes to construct a more informative picture of the behavior of the induced magnetic field of a molecule. In this case, however, the probes are placed at 0.1 Å intervals along a line that traverses the length of system (usually a symmetry element) at a constant height. Assuming the molecule is placed in the *XY* plane, this means the trajectory of NICS probes is also parallel to the *XY* plane, hence the name of the method. The NICS-*XY*-Scan method can be used with any type of NICS metric, though we advocate for using $\mathrm{NICS}(1)_{\pi ZZ}$ when possible. When this is computationally too expensive, a good compromise is $\mathrm{NICS}(1.7)_{ZZ}$. The height of 1.7 Å was shown to provide qualitatively similar results to the more expensive dissected version (Figure 12).

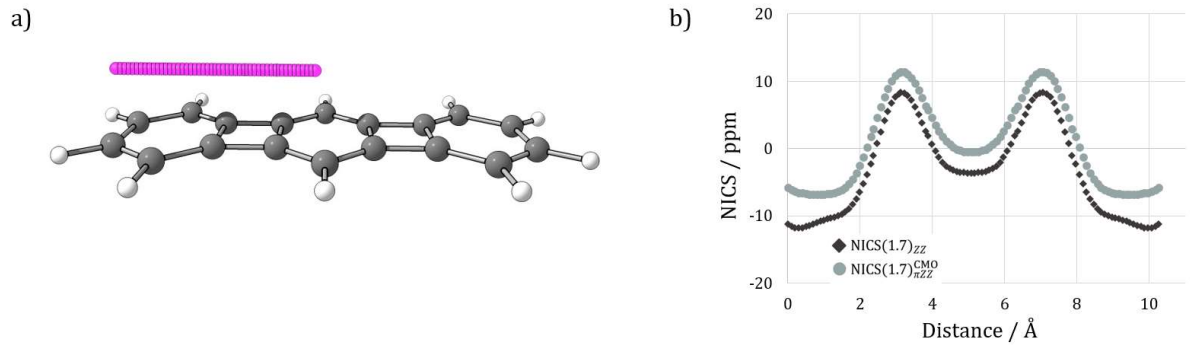

Figure 12. NICS-XY-Scan of [3]phenylene: a) visualization of the molecular structure and placement of the NICS probes (only one half is necessary, the results can be mirrored for the other half); b) plot of NICS values versus the distance of the scan (gray – $NICS(1.7)_{\pi ZZ}$; black – $NICS(1.7)_{ZZ}$). The NICS values were calculated with Gaussian 09 using the GIAO method and the B3LYP/6-311+G(d) level of theory.

As with all NICS-based methods, the NICS-*XY*-Scan is also rather user-friendly to run. The resulting “aromatic profile” can be used to identify different types of ring currents within a system. To the best of our knowledge, the NICS-*XY*-Scan is the only reliable NICS-based method for assessment of aromaticity in polycyclic systems. We note that one can consider the “local aromaticity” approach, i.e., calculating NICS values at or above the center of the rings, as a very sparse NICS-*XY*-scan trajectory. This type of analysis gives part of the information, but due to the sparseness of the probes, it does not fully describe the ring current(s), and this may lead to misinterpretations in some cases. The example of [3]phenylene in Figure 12 is a simple one, where the neighboring ring have distinct character. In such a case, a single point would give the same interpretation—alternating aromatic and antiaromatic rings. Other cases can be harder to interpret. One such example is pentalene (**4**) and its dication (**5**). Pentalene is an 8π-electron bicyclic antiaromatic molecule, and pentalene diaction is the corresponding 6π-electron aromatic molecule. Both compounds are symmetric and a $\mathrm{NICS}(1.7)_{ZZ}$ calculation shows, unsurprisingly, identical values for the two rings within each compound: 58.1 ppm for the pentalene rings and -29.6 ppm for the pentalene

dication rings. This could be interpreted either as both rings having the same local ring current, or both being encompassed by the same global ring current. From the single NICS values we cannot distinguish between these two scenarios, but the NICS-*XY*-Scans shed more light. As seen in Figure 13a and b, they show that neutral pentalene has a "two-shoulder" profile, i.e., two clear maxima. Pentalene dication has a different shape, which looks more like a plateau (for the $\mathrm{NICS}_{\pi ZZ}$ values) or a dip (for the NICS_{ZZ} values) between the centers of the two rings—not two extrema points. As described by Stanger, Monaco, and Zanasi,[63] these different shapes are characteristic of ring current topologies and point to different behaviors. The "two-shoulder" case indicates local ring currents while the plateau/single extremum indicates a global ring current. These conclusions are corroborated by the respective current density maps (Figure 13c and d). Several additional examples, as well as a set of guidelines for interpretation of NICS-*XY*-Scans, are given in Reference 63. Note, also, how the qualitative analysis is made possible with either the dissected NICS metrics or with the $\mathrm{NICS}(1.7)_{ZZ}$ metric.

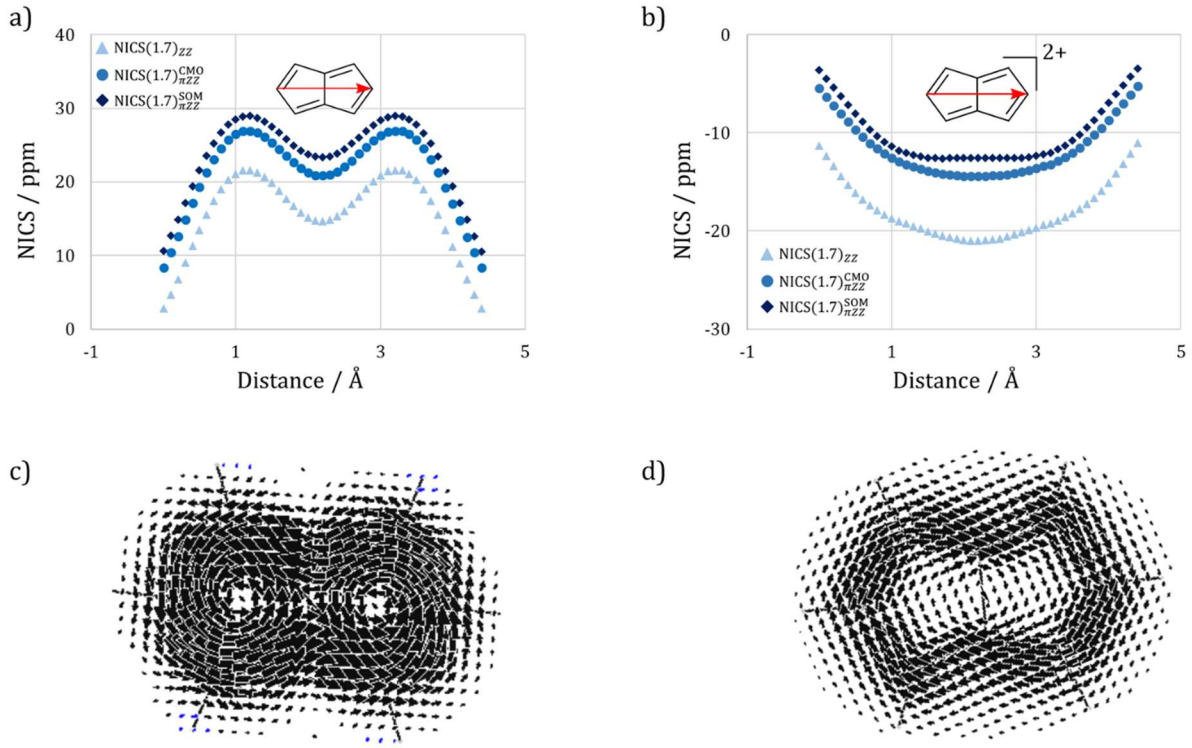

Figure 13. Comparison of NICS-XY-Scans of a) pentalene and b) pentalene dication. Comparison of current density maps of c) pentalene and d) pentalene dication. Geometries optimized with Gaussian 09 at the B3LYP/6-311G(d,p) level of theory. NICS calculated with GIAO and the B3LYP/6-311+G(d) level of theory. Current density maps calculated with SYSMOIC.

The NICS-*XY*-Scans also introduce the ability to study polycyclic molecules along more than one pathway. The number of NICS-*XY*-Scans depends on the symmetry of the system. For example, for pyrene we used two scans (in a subsequent section below we also show three scan pathways for coronene).[62] The scans bisect the molecule along each of the two main symmetry axes, enabling characterization of the two types of rings as well as identification of the global pyrene current (Figure 14).

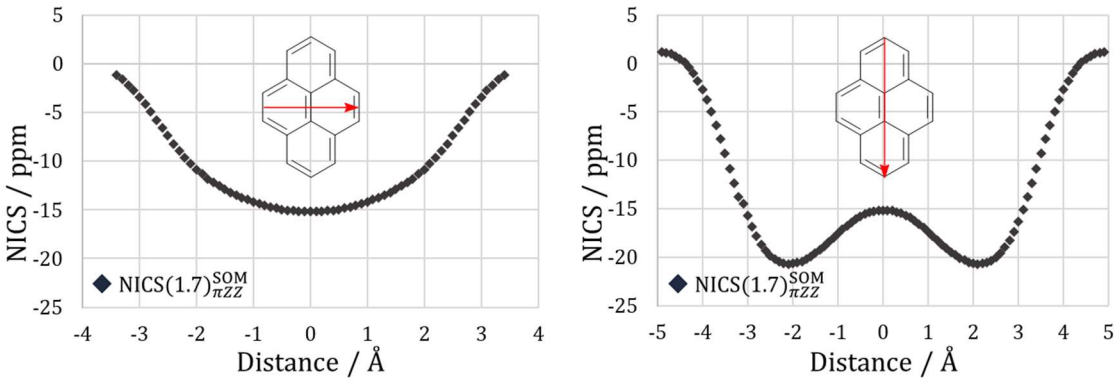

Figure 14. NICS-XY-Scans for pyrene. In each panel, the scan pathway is denoted by a red arrow. The NICS values reported are NICS(1.7)$_{\pi ZZ}$ values, obtained with the σ-Only Model, calculated with Gaussian 09 using the GIAO method and the B3LYP/6-311+G(d) level of theory.

Though we recommend NICS-XY-Scans for examination of polycyclic aromatic systems, we caution that no procedure (either NICS-based or not) has been developed yet to quantify the aromaticity of polycyclic systems. This remains an open challenge, as it is not even clear how one would define the aromaticity of a polycyclic system, given these systems’ tendency to contain areas with different character.

In 2018, Gershoni-Poranne showed that the NICS-*XY*-Scans of *cata*-condensed polycyclic systems containing four rings or more can be predicted using an additivity scheme.[64] The predictive method demonstrates that the larger systems can be constructed as superimposed sums of the smaller subunits that they contain, up to tricycles. As a result, the NICS-*XY*-Scans of much larger systems can now be generated at a high level of theory with very inexpensive calculations. The additivity method has been shown to work also with heterocycle-containing *cata*-condensed polycyclic systems.[65]

NICS Methods for Macrocyclic Systems

NICS is often used for the characterization of macrocyclic polyaromatic systems. One should remember that NICS was originally developed for monocyclic systems, and such macrocyclic systems are far beyond the scope of the original methodology. Nevertheless, NICS-based characterization of these systems has become common practice and will most likely remain so in the coming years, thus they warrant discussion in the scope of this chapter.

Some examples include the work of Wu and coworkers[66–68] and Anderson and coworkers (Figure 15).[69–72] While these are also polycyclic aromatic systems, they are different from the *peri*- or *cata*-condensed molecules normally studied with NICS indices. In such cases as the Anderson poly-porphyrin nano-rings or the Wu cages, discussion revolves around “global aromaticity”. Measuring currents with such topologies and in such complex systems is challenging for many reasons. Technically, they require significant computational resources to calculate at a comparable level. With these larger systems, it may become more difficult to employ these more expensive methods. Additionally, conceptually, one encounters the dilemma of choosing the appropriate method and the appropriate location for the NICS probes. What would we consider the out-of-plane axis to be? Is it perpendicular to each of the rings in turn, or is it the axis of highest symmetry for the entire system? In addition, there is no way to perform a 1D scan, as it would “crash into” another part of the system.

In 2015, the S-NICS[73] method was proposed by Monajjemi and Mohammadian for characterization of nanomolecules. This is a statistical method that used NICS probes in spheres of shielding and deshielding spaces of molecular rings over short and long distances. Using Monte-Carlo statistical calculations, they calculated the skew and asymmetry parameters and defined a new criterion, termed *modified isotropy*, which arises from the maximum abundance of states. According to the description given by the authors, the main advantage of the S-NICS method is that it is not dependent on the shape and structure of the molecule or its center. Yet, as they clearly state, it “would be lengthy without using any simplifying software” and “is not simple compared to NICS” This may explain why, to the best of our knowledge, this method is not widely used. Rather, the method of choice for macrocyclic systems appears to be $\mathrm{NICS}(0)$ isosurfaces. These were also used in the examples of Anderson and Wu referenced above. One example is shown in Figure 15, where the $\mathrm{NICS}(0)$ isosurfaces are used to characterize the aromaticity of poly-porphyrin macrocycles with different charges. As can be seen, the neutral system has small NICS values (in absolute value) which seem to be localized around the porphyrins. The tetra-anionic system had strong positive NICS values in the center of the macrocycle and negative NICS values outside the macrocycle, indicating a global paratropic current. For the hexa-dianionic system, this is reversed.

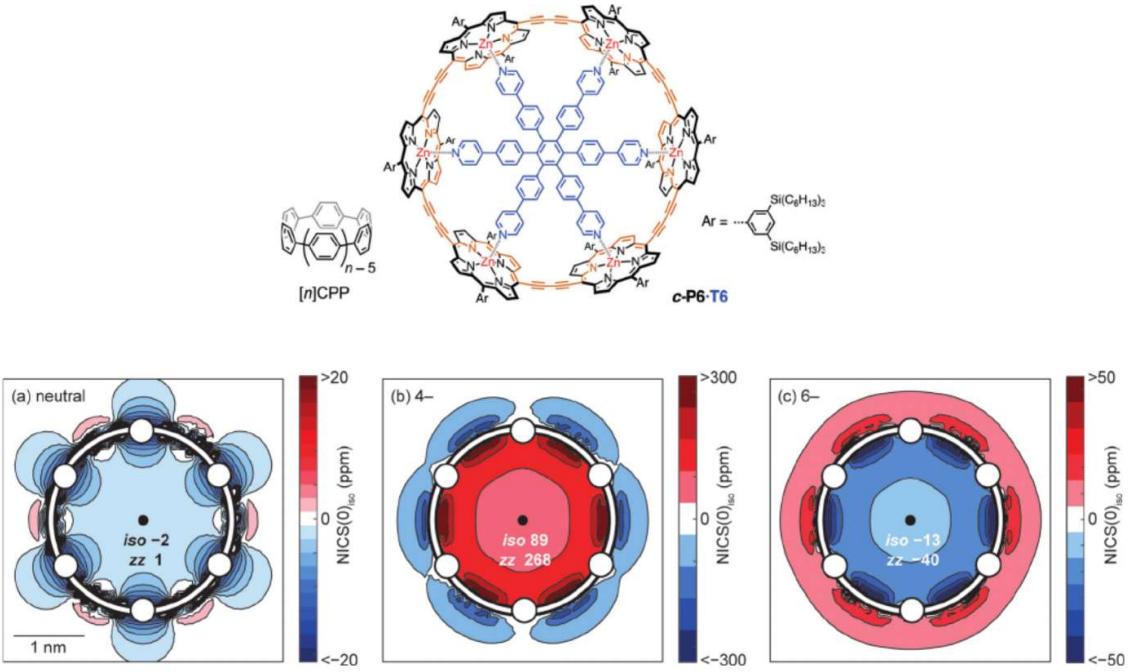

Figure 15. NICS isosurfaces from Anderson and coworkers’ poly-porphyrin anionic macrocycles. Top: structure of poly-porphyrin macrocycle; Bottom: NICS(0) isosurfaces of poly-porphyrin macrocycles with various charges, a) neutral, b) charge = -4, c) charge = -6. Reprinted with permission from Reference [72].

Though we generally strongly recommend against using $\mathrm{NICS}(0)$, in cases such as these, a separation of π and σ orbitals is very difficult (or effectively impossible) to achieve. Thus, one cannot calculate $\mathrm{NICS}(r)_{\pi}$. Altogether, considering the challenges posed by these systems, an isosurface of $\mathrm{NICS}(0)$ appears to be the best, and most informative, description one can provide. Nevertheless, we believe that the interpretation of these results should be done with the utmost care and should not be benchmarked

against more “traditional” aromatic systems. Rather, the data for these compounds should be considered only within the context of other, similar geometries.

The Importance of Dissected NICS

Aromaticity, in the classical sense, is a π-system property (in the next section we provide examples of how it has moved beyond conventional π-systems). Thus, when applying magnetic criteria-based techniques for evaluating aromaticity, it is important to distill out the π-effects from all other effects. Failure to do so may result in erroneous results and/or misinterpretations. In the preceding section we introduced the “dissected NICS” methods, which do so, by considering only the π-electron contributions to the chemical shift tensor. The dissection can be achieved with NBO or with the σ-Only Model, and affords the metrics known as $\mathrm{NICS}(r)_{\pi}$. Note: considering in addition only the *ZZ* component of the chemical shift tensor would further refine this to $\mathrm{NICS}(r)_{\pi ZZ}$, which is often considered the state-of-the-art of NICS-based methods.

In this section, we aim to underline the importance of this dissection procedure for correct interpretation of aromatic character. To this end, we study the example of coronene. Three types of NICS metrics (isotropic $\mathrm{NICS}(1)$, $\mathrm{NICS}(1)_{ZZ}$, and $\mathrm{NICS}(1)_{\pi ZZ}^{\mathrm{CMO}}$) were used to calculate three NICS-*XY*-Scans: a) horizontal “*X*-scan”, b) a vertical “*Y*-scan”, c) a peripheral ”Peri-scan”. For clarification, we have omitted the double bonds and have labeled the rings with black capital letters A-G and bonds through which the pathways go with gray lowercase letters a-h (Figure 16).

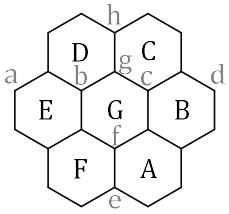

Figure 16. Schematic depiction of coronene and the notation of rings and bonds as described in the text.

The results of these are shown in Figure 17.

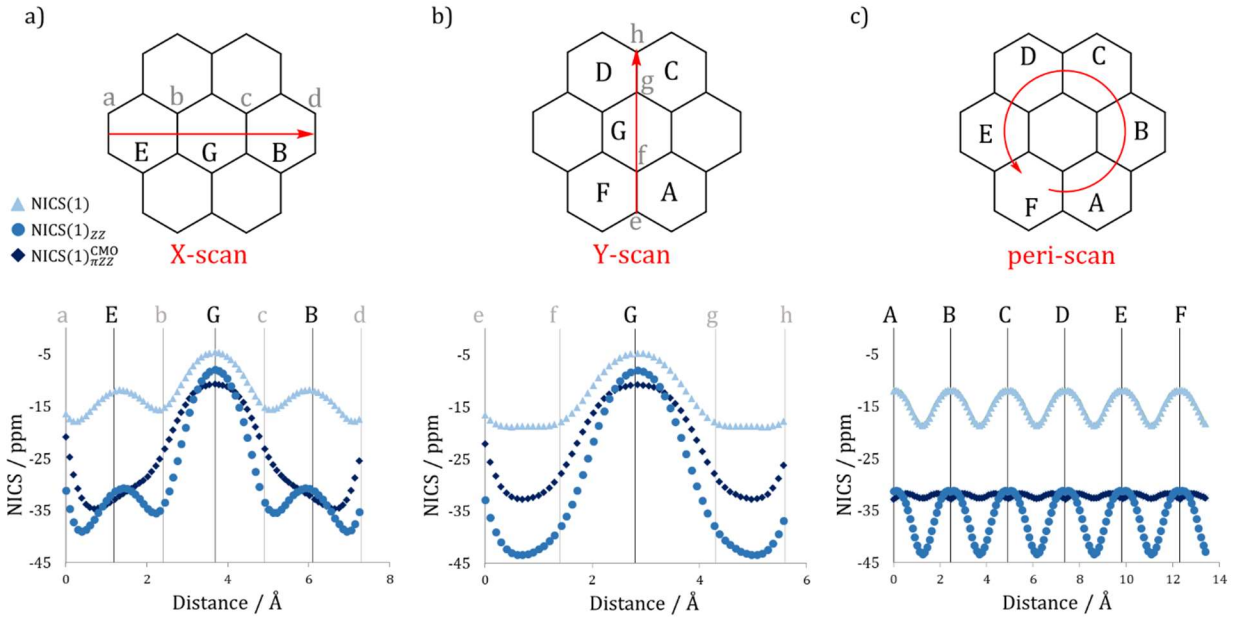

Figure 17. NICS-XY-Scans of coronene, top: scheme of molecule and scan pathway, bottom: plot of NICS-XY-Scans with isotropic $NICS(1)$ (light blue), $NICS(1)_{ZZ}$ (blue) and $NICS(1)_{\pi ZZ}^{CMO}$ (dark blue) metrics. A) horizontal “X-Scan”; B) vertical “Y-Scan”; c) Peripheral “peri-Scan”.

The three NICS methods give qualitatively different pictures of the aromatic character of coronene. The isotropic $\mathrm{NICS}(1)$ metric shows a relatively weak global diatropic current with weak local paratropic currents in each of the six-membered rings. The $\mathrm{NICS}(1)_{\mathrm{ZZ}}$ metric indicates a much stronger global diatropic current and a considerably strong paratropic current in the central ring and weaker paratropic currents in the peripheral rings. The most refined NICS metric, $\mathrm{NICS}(1)_{\pi\mathrm{ZZ}}^{\mathrm{CMO}}$, shows a strong global diatropic current around the peripheral rings and, again, a medium-intensity paratropic current in the central ring. In contrast to the less refined methods, it shows no paratropic currents in rings A-F. The small minima seen in

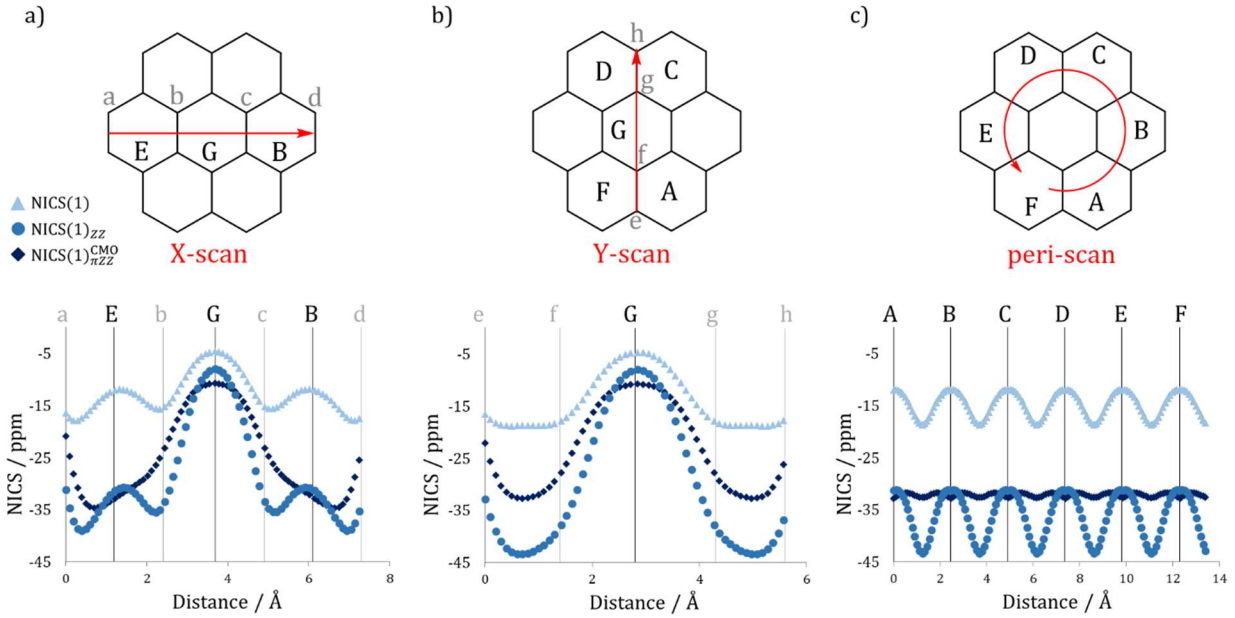

Figure 17c above each “spoke” bond (the fused bonds between neighboring rings in the periphery) and above each ring center indicate small diatropic currents above these C-C bonds and ring centers.

These results agree with the pictures obtained from current density analysis calculations (Figure 18).

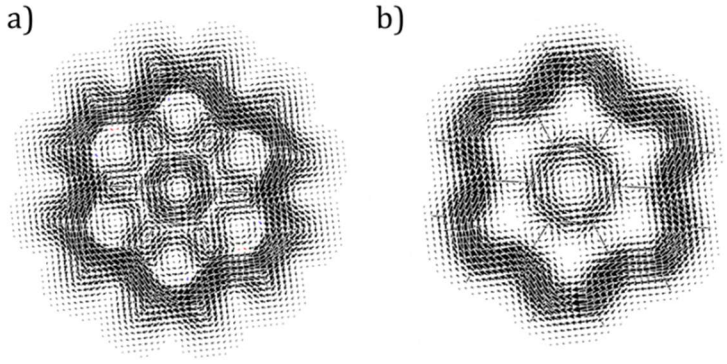

Figure 18. Current density maps of coronene obtained with a) contributions of all electrons and b) only π-electrons.

The differences between the three “levels” of calculation highlight the importance of dissection. The interpretation is substantially different when the contributions of non-π electrons are included in the NICS calculation.

To demonstrate the apparent differences of analyzing the system with the isotropic $\mathrm{NICS}(1)$ metric, we calculate the difference $NICS(1) - NICS(1)_{\pi ZZ}^{CMO}$. These plots are meant to underline the numerical differences between the methods and how using the isotropic metric can change our understanding of the aromatic character of the system. Figure 19 shows the plots corresponding to the three scan pathways. As can be seen from the plots, in all cases the isotropic value is less negative, indicating a weaker ring current. In the peripheral rings, the isotropic NICS value gives a values 21 ppm higher than $\mathrm{NICS}(1)_{\pi Z}^{\mathrm{CMO}}$. The “zig-zag” pattern in panel c is similar in pattern and amplitude to the one seen in Figure 17c, which suggests this is indeed an effect of the σ-electrons. However, the absolute values are much higher, which leads to an overall much smaller NICS value. These differences have a marked effect on the current picture and, hence, the interpretation of aromatic character.

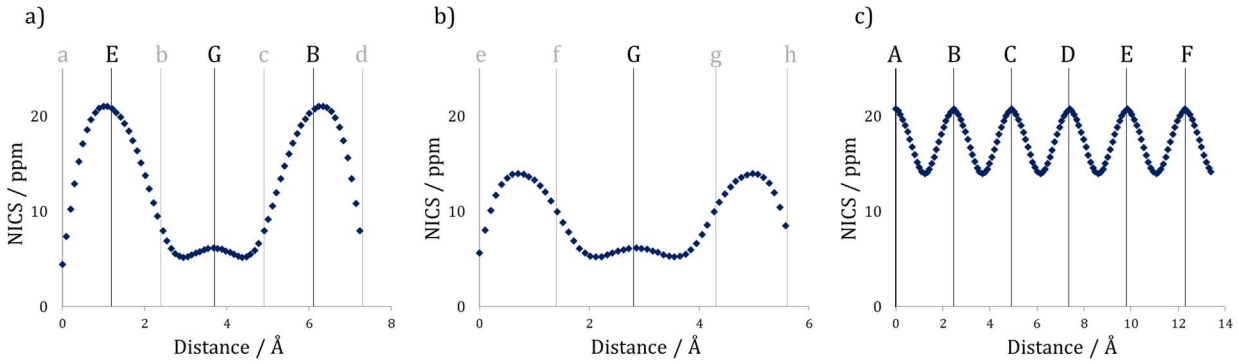

Figure 19. NICS-XY-Scans of coronene for the difference $\left[NICS(1) - NICS(1)_{\pi ZZ}^{CMO}\right]$ *. A) horizontal “X-Scan”; B) vertical “Y-Scan”; c) Peripheral “Peri-Scan”.*

Another way to illustrate the effect of non-π electrons is to calculate what percentage of the isotropic NICS value is from the $\mathrm{NICS}(1)_{\pi ZZ}^{CMO}$ (Figure 20). As the plots show, 90% of the isotropic value above the centers of the peripheral rings is contributed by the $\mathrm{NICS}(1)_{\pi ZZ}^{CMO}$. However, above the central ring, this decreases to 80% and above the spoke bonds it further drops to 60%. In the "*Y*-scan" we see that as much as 55% of the isotropic NICS value does not come from the $\mathrm{NICS}(1)_{\pi ZZ}$.

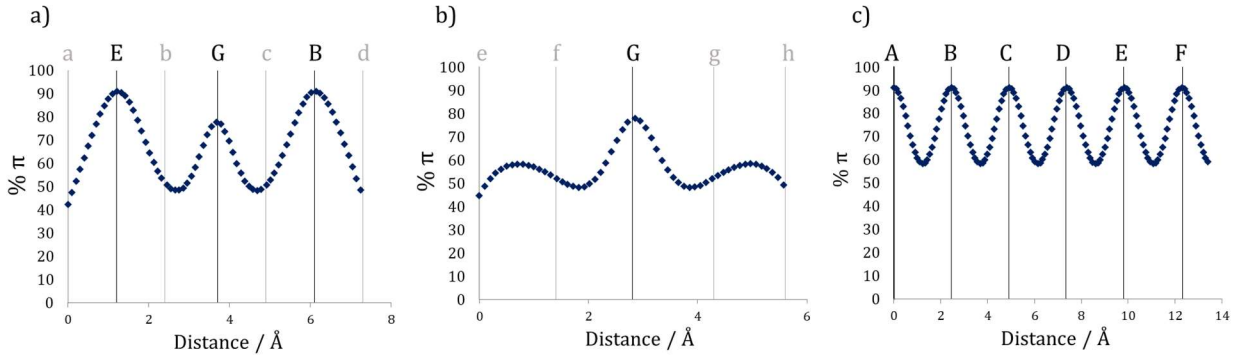

Figure 20. NICS-XY-Scans of %$NICS(1)_{\pi ZZ}^{CMO}$ of the isotropic value . A) horizontal "X-Scan"; B) vertical "Y-Scan"; c) Peripheral "Peri-Scan".

All of these serve to emphasize that the isotropic NICS metrics contain significant contributions from non-π electrons. This leads to quantitatively incorrect evaluation of aromaticity, and may also lead to qualitatively wrong assignation of aromaticity.

It is often assumed that taking only the *ZZ* component of the chemical shift tensor is enough to mitigate this problem. By calculating the difference $NICS(1)_{ZZ} - NICS(1)_{\pi ZZ}^{CMO}$ we show that this is not the case. This difference effectively affords the contribution of the non-π electrons to the *ZZ* component of the chemical shift tensor. The three plots in Figure 21 show this difference for the three NICS-*XY*-Scan pathways described above. As can be seen from the plots, the σ-electrons are responsible for the dramatic "zig-zag" shape seen in Figure 17c, due to their slightly paratropic contributions above the ring centers and slightly diatropic contribution above the fused bonds. Also, though they contribute up to -11 ppm (i.e., approximately 20%) of the diatropicity found above the spoke bonds in the vertical "*Y*-scan", their contribution to the paratropicity of the central ring is minimal. Meaning, this paratropic behavior does indeed come from the π-system. On the other hand, the "bumps" seen in the two peripheral rings in the horizontal "X-scan" are the source of the (erroneous) interpretation of small paratropic currents in these rings. Seen in this light, it becomes clear that this is an artefact and not a π-system property.

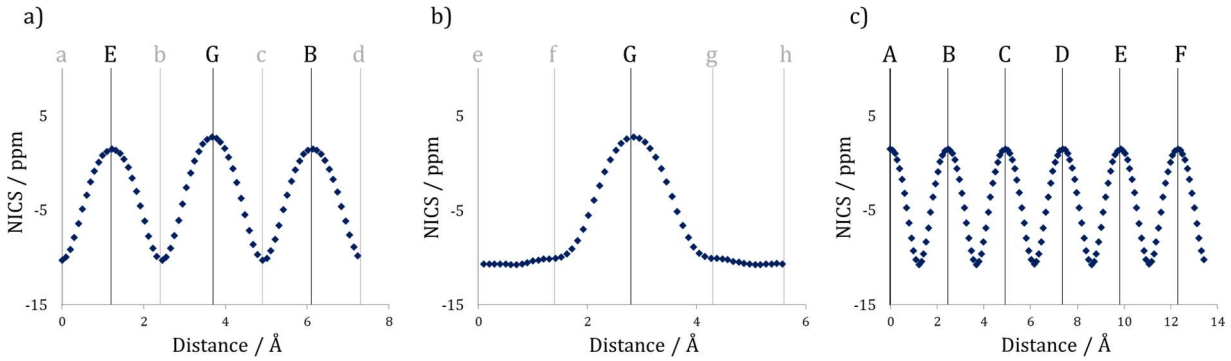

Figure 21. NICS-XY-Scans of coronene showing the contribution of the σ-electrons to the ZZ componenet of the chemical shift tensor, calculated as $[NICS(1)_{ZZ} - NICS(1)_{\pi ZZ}^{CMO}]$ *. A) horizontal “X-Scan”; B) vertical “Y-Scan”; c) Peripheral “Peri-Scan”.*

The analysis presented here demonstrates that using un-dissected NICS metrics can lead to wrong interpretations of the aromatic character of a system, and that taking only the *ZZ* component of the chemical shift tensor is not sufficient to ensure a “clean” π-electron evaluation. It is therefore important to use $\mathrm{NICS}_{\pi ZZ}$ whenever possible. When this cannot be done, $\mathrm{NICS}(1.7)_{ZZ}$ is a relatively safe alternative, because the contribution of the non-π electrons is almost constant at this height. Thus, while the values may be different, the important features of the shape of the plot should remain clear.

NICS Beyond π-Systems

The term “aromaticity” was born from the realm of cyclically conjugated π-systems and has been applied to such compounds for over 150 years. However, the concept has long since been expanded to include systems other than the prototypical organic, π-conjugated compounds. This is exemplified in terms such as hyperconjugative aromaticity, homo-aromaticity,[74] super-aromaticity,[75] carbo-aromaticity,[76,77] metallo-aromaticity,[78,79] and more (for a recent review of unconventional aromaticity, see the account by Zhu and coworkers).[80] The notion that such systems are aromatic, and exactly what kind of aromaticity they might have, are topics that are somewhat controversial and have been debated in the literature. To be clear, we do not intend to review here these fundamental issues or their validity. In keeping with the main theme of our overview, we focus on the application of NICS-based methods to such systems and describe potential pitfalls. For each of the categories listed above, we give a brief description of the term, refer the reader to relevant literature for further reading, and describe general guidelines for using NICS-based methods. Importantly, these systems present similar challenges for NICS as those described above for π-conjugated system, but also introduce new difficulties that must be considered.

Hyperconjugative aromaticity is the notion that a non-conjugated molecule can become aromatic due to the participation of non-p orbitals (usually, σ_{CX} orbitals) in the π-system *via* hyperconjugation (Figure 22).

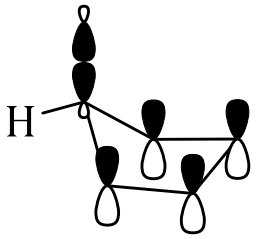

Figure 22. Orbital interactions enabling hyperconjugative aromaticity. The participation of the out-of-plane σ_{CX} orbitals via hyperconjugation creates a cyclically conjugated system.

It is often invoked with respect to cyclopentadiene,[40,81–83] though other cyclopolyenes have been discussed.[84] The significance of the effect is manifested in stereochemical as well as kinetic consequences, as it has been shown that selectivity and rate (e.g., for cycloaddition reactions)[81] can vary depending on the substituent on the saturated carbon. The use of NICS for such cases was initiated by Schleyer’s claim of hyperconjugative aromaticity in cyclopentadiene, however, it was subsequently disputed by Stanger[41] who claimed that this stemmed from a misinterpretation of the single-point NICS values calculated by Schleyer. Based on multi-point NICS methods, as well as other criteria of aromaticity, Stanger argued that these systems are not aromatic. The topic remains unresolved, with reports supporting both arguments. For example, in 2009 Alonso and Herradon used a neural network trained on multiple aromaticity criteria to investigate substituent effects on cyclopentadiene and cyclopentadienyl anion.[85] For both families of compounds, they observed that the aromaticity of the five-membered ring decreases, regardless of the electronic nature of the substituent. This would appear to contradict the hyperconjugative aromaticity argument, according to which the nature of the substituent should affect the amount of hyperconjugation. On the other hand, in 2015 Levandowski and Houk published a computational study that investigated the reactivity of 5-substituted cyclopentadienes in Diels-Alder reactions with ethylene and maleic anhydride.[81] They claimed that the substantial increases in rate constants for certain compounds have a direct relationship to their hyperconjugative aromaticity. This serves to demonstrate that, as with “regular” aromatic molecules, the same caution (or even more) must be used for hyperconjugative aromaticity. This is especially true because the values obtained for such compounds are expected to be smaller, and hence, more ambiguous for interpretation. To avoid such misinterpretations, we recommend, again, choosing the more refined NICS versions in combination with multi-point techniques, as well as benchmarking against similar systems (not only against prototypical aromatic structures). We also note that attention has been focused mainly on the effect that substituents have on the extent of hyperconjugative aromaticity. For main-group elements, the standard recommendations still apply, however, many of the studied substituents are heavy atoms, for which these methods are generally not suitable. This is expanded upon below, where we discuss inorganic systems.

Homoaromaticity, similarly to hyperconjugative aromaticity, refers to systems in which an sp^3-hybridized atom interrupts an otherwise conjugated π-system. Though on the face of it, this would appear to disrupt aromaticity, these systems do exhibit many of the characteristic behaviors of aromatic compounds (e.g., magnetic, spectroscopic, energetic). This is explained by the formation of a continuous overlap of p-orbitals, which is obtained by a geometric distortion that pushes the saturated carbon out of the plane and brings the two adjacent sp^2 carbon atoms closer to each other. One well-known example of homoaromaticity is the homotropylium cation (Figure 23).

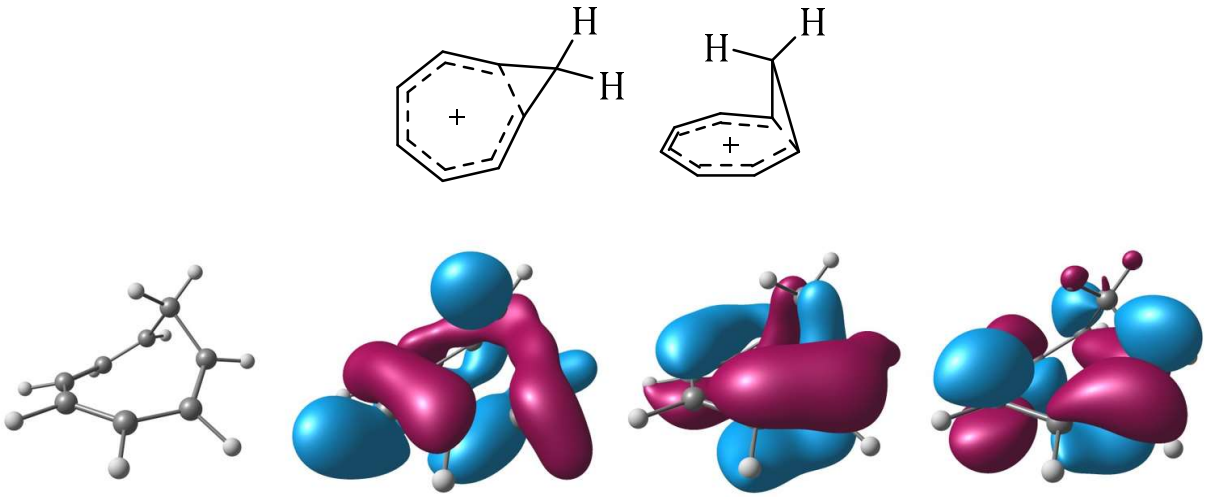

Figure 23. Top: Schemes of homotropylium. Bottom: calculated structure of homotropylium and three representative MOs demonstrating the π-like continuous cyclic overlap of orbitals achieved by distortion of the saturated carbon out of the plane of the ring. Geometry optimized at the B3LYP/6-311G(d,p) level of theory with Gaussian 09, orbitals visualized at the isosurface value α = 0.04.

Since these systems are generally hydrocarbon-based, they do not encounter the difficulties of inorganic systems (see below). However, they are inherently non-planar. Therefore, one needs to consider carefully where to place the NICS probe(s). Assuming the distortion places the extruded group on one side of the ring plane, obviously, the (series of) probe(s) should be positioned on the opposite face. Nevertheless, it is important to recognize that, due to the non-planarity of the system, CMO- or LMO-based dissected NICS cannot be used. Additionally, though the σ-Only Model can in principle treat non-planar systems, in these cases it may be difficult (or even impossible) to place the hydrogens. Therefore, it is likely that the most refined NICS metric possible will be $\mathrm{NICS}(1)_{\mathrm{ZZ}}$ or $\mathrm{NICS}(1.7)_{\mathrm{ZZ}}$, which can be obtained as a single-point calculation or with a NICS-Scan

Super-aromaticity describes global ring currents that are generated in a cyclic array of benzene (or benzenoid) rings. Some examples of structures that may sustain such currents are kekulene,[86–88,26] cycloarenes,[89] nano-rings, and carbon nano-toroids[90] (Figure 24). Note that super-aromaticity is distinct from global aromaticity in macrocycles, which we discussed previously.

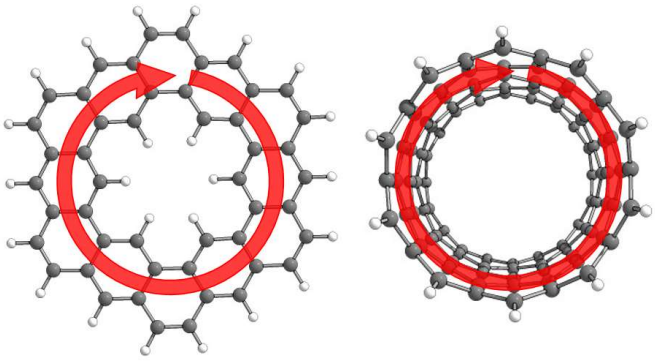

Figure 24. Schematic depiction of the expected ring currents in super-aromatic kekulene (left) and a super-aromatic carbon nanotube (right).

In this long-standing debate whether, in fact, these systems are super-aromatic,[75] NICS-based methods have often been used to characterize the compounds under investigation. For such polycyclic systems, a single NICS calculation is clearly insufficient. We recommend using NICS-*XY*-Scan(s) to characterize the system. As shown above for pyrene and coronene, more than one NICS-*XY*-Scan may be needed, in order to obtain a good description of all types of rings in the system. As always, we recommend the $\mathrm{NICS}(1)_{\pi\mathrm{ZZ}}$ metric. If it is not possible to calculate a NICS-*XY*-Scan, at the very least, NICS values must be calculated for each type of ring. These approaches may be used for planar *peri*-condensed systems, but they are not easily applied to nano-rings and nano-toroids. The geometries of these systems often preclude dissected NICS methods, and multi-point NICS methods may also be impossible. In such cases, a reasonable alternative is the $\mathrm{NICS}(1.7)_{\mathrm{ZZ}}$ metric. Regardless of the NICS metric chosen, we emphasize that these systems often have complex magnetic behavior, which NICS may struggle to describe. For example, in carbon nano-tubes, super-aromaticity depends on the number of poly-benzene "rows", as well as the direction of the applied field (parallel or perpendicular to the nano-tube).[91]

Carbo-aromaticity is a term dedicated to the class of carbo-mers—cyclically conjugated molecules consisting of alternating triple bonds and/or cumulenes (Figure 25).[77]

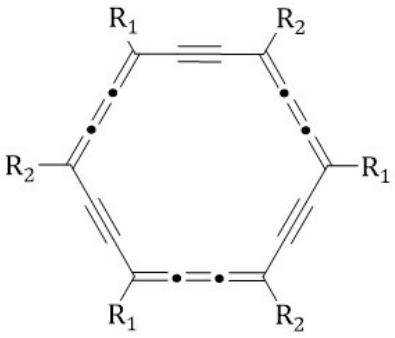

$R_1 = H$; $R_2 = Ph^tBu$
$R_1 = Ph$; $R_2 = Ph$ or Ph^tBu
$R_1 = {}^t\mathrm{Bu}$; $R_2 = Ph$

Figure 25. Heptacyclic carbo-benzene reported by Chauvin and coworkers

The natural choice for placing the NICS probe in these cases is at the geometric center of the macrocycle. Contrary to "regular" aromatic systems, σ-contaminations are likely to be negligible at this location, because of the larger radius of the macrocycle. Hence, one may choose to forgo the requirement to raise the probe above the molecular plane. Yet, for the same reason, the values obtained cannot be easily compared to values obtained in benzenoid systems. As the distance between the NICS probe and the circumference increases, the induced field felt by the probe weakens. This does not mean, however, that the induced ring current is weaker. Thus, the main challenge here is in obtaining chemical insight. While the technical application of NICS is simpler than in the aforementioned cases, careful and appropriate benchmarking should be undertaken when interpreting these results.

Finally, we consider metallo-aromaticity, which refers to aromaticity in systems containing or entirely made of metal atoms; i.e., organometallic compounds and all-metal clusters, respectively. In contrast to the previous cases, these inorganic aromatic systems encompass a significantly larger field of research. A comprehensive book chapter on these systems was written by Popov and Boldyrev in 2014,[92] to which we refer the reader for further reading. Inorganic systems have been studied with NICS quite extensively. Some examples include silabenzenes,[93] annulated borepins,[94,95] B- and BN-containing systems,[96–100] BP-containing sytems,[101] phosphorous heterocycles,[102] and Group 14 organometallics[103] and metalloles.[104]

Additionally, comprehensive collections of data have been reported for series of monocyclic planar inorganic compounds by Geerling and coworkers[105] and by Solà and coworkers.[106] Maslowsky has provided a very informative review on the aromaticity of metallacenes—sandwich compounds of transition elements with inorganic rings.[107]

The aromaticity of all-metal aromatic compounds was previously reviewed by Boldyrev and Wang[108,109] and, separately, by Tsipis.[110] For our purposes, we note some examples of all-metal and semi-metal clusters that have been characterized with NICS-based methods, including cyclic alkali clusters,[111] boron-hydride clusters,[112] coinage-metal clusters,[113] and uranium clusters.[114]

The types of NICS-based methods used in the reported studies vary widely, from $\mathrm{NICS}(0)$ to $\mathrm{NICS}(1)_{\pi}$ and $\mathrm{NICS}(1)_{\mathrm{ZZ}}$. Solà and coworkers tested NICS-based method for a series of all-metal and semi-metal clusters (containing only light metals, not transition metals) and compared the results to other indices of aromaticity. They found that $\mathrm{NICS}(0)_{\pi}$ is a reliable metric for quantitative study of such systems, but $\mathrm{NICS}(0)$ and $\mathrm{NICS}(1)$ are not. They did not test the $\mathrm{NICS}(1)_{\pi}$ metric, so it is unknown if it would perform comparably to or better than other metrics. Tiznado and coworkers later suggested a new NICS-based method to minimize the misinterpretations that can arise in inorganic heterocycles.[115] Their method, called *free of in-plane component NICS* (FiPC-NICS) combines features of previously reported NICS-based methods. The user first performs a NICS-Scan on the molecule and plots the out-of-plane and in-plane components of the NICS values at each distance point against each other. The height where the in-plane component decays to zero is chosen as the FiPC-NICS point, and the out-of-plane component at that height is reported as the evaluation of aromaticity. The rationale is similar to the original idea of raising the NICS probe to eliminate σ-contaminations: we wish to identify a point in space where the induced magnetic field is stems mainly from aromaticity or antiaromaticity and is free from other contaminations. The difference here is that the height of the reported NICS value varies between different molecules. As an added layer of interpretation, the authors consider the shapes of the plots to indicate characteristic aromatic/antiaromatic/nonaromatic behavior. FiPC-NICS has been used to evaluate several cases of planar systems, including some monocyclic prototypical structures[38] and heterocyclic benzene analogues. In our view, the underlying principle of FiPC-NICS is correct, in that it aims to obtain the clean effect of the π-electrons on the out-of-plane NICS value, and it circumvents the need for computational separation of σ- and π-electron contributions. In addition, the use of characteristic plot shapes helps to avoid misinterpretations. However, it should be noted that, in practice, this method evaluates different molecules at different heights, depending on where their in-plane components decay to zero. Since the out-of-plane component also decays with height, and the decay rate is not identical for all systems, this means that the results are not comparable across different systems. In general, our recommendations are in line with those from these reports.[116] For cyclic molecules containing smaller atoms (e.g., B, N), $\mathrm{NICS}(1.7)_{\mathrm{ZZ}}$, $\mathrm{NICS}(1)_{\pi\mathrm{ZZ}}$, and $\int \mathrm{NICS}$ are all satisfactory metrics. FiPC-NICS can be used to compare systems where the height at which the value is determined is similar.

For cyclic molecules containing larger atoms (Si, Ge, etc.), raising the probe 1 Å above is often insufficient since, even at this height, the probes are within the range of the orbitals of the larger atoms. In addition, these systems are often non-planar, making the separation of the out-of-plane component difficult, and the identification π-orbitals' (or δ-orbitals') contribution to the chemical shift effectively impossible. Similarly, for clusters, it is not clear where one should place the probe, and how different clusters can be compared, when they have significantly different sizes, number of electrons, and locations of NICS probes. Yet even if this dilemma could be solved, another important issue remains, which is the incorporation of

heavier atoms and transition metals. As pointed out by Foroutan-Nejad et al. in a recent publication,[117] NICS cannot distinguish between effects stemming from ring current and the local paramagnetic effects of heavy elements on their neighboring atoms. This is also true for all-metallic clusters. In the past, these had been considered to sustain ring currents, and were thus characterized as having magnetic aromaticity. However, further research revealed that the reported NICS values actually stemmed from strong local paratropic currents.[118] There are some additional reports documenting the problems with applying NICS to such molecules.[119,120] In light of the combined technical and interpretational difficulties, our recommendation is not to use NICS to study the aromaticity of molecules containing heavy atoms and/or transition metals.

How NICS Compares to Other Indices

The comparison of NICS to other methods can be done on several levels: *accuracy*, *reliability*, and *ease of use*.

We start with the third criterion. Without a doubt, NICS is exceptionally easy to use. Not only is it conceptually easy to understand, it is also technically easy to implement with available software, such as Gaussian,[32] GAMESS,[121,122] ORCA,[33,34] or ADF.[123] Since 2014, this has been made even easier with the development of the Aroma software by Rahalkar and Stanger.[124,47,36,62] This free program automates the preparation of input files for Gaussian for calculation of NICS, NICS-Scans and NICS-*XY*-Scans, and offers as well two dissection methods: CMO and the σ-Only Model. Following the calculation, Aroma also extracts the relevant data from the output files and provides the user with the final values requested.

In terms of accuracy, as a computational method, the obtained NICS values are as accurate as the level of theory employed. Certain choices lead to better accuracy, for example, using a larger basis set, including polarization and diffuse basis functions and using dense integral grids. In general, NICS values are considered to be accurate to about ±2 ppm.

The reliability of NICS is perhaps the most controversial aspect—is a NICS-based assignation of aromatic/anti-aromatic/non-aromatic character reliable? This question relates to the choice of NICS version and the interpretation of the results.

As mentioned above, aromaticity is a difficult property to evaluate because it cannot be measured or calculated directly. As a result, it is defined by convention, usually in reference to a prototypical compound—such as benzene or cyclobutadiene—and an artificial reference state. This means that, very often, in order to convincingly determine the aromatic character of a compound, its aromaticity is evaluated with several metrics, and these are compared. In simple cases, there is an overwhelming agreement between all (or most) indices, and there can be a consensus about the characterization of the compound. In other, more perplexing, cases different indices provide differing conclusions. There have been cases of NICS values contradicting other indices of aromaticity and, for several years, this was attributed to the "multidimensional character" of aromaticity.[125–127] However, as Solà summarizes in his essay "Why Aromaticity is a Suspicious Concept? Why?",[128] further investigations have shown that these discrepancies are often due to the fact that certain indices do not measure aromaticity accurately (or correctly). As we have seen above, some of the earlier NICS metrics themselves are not good indicators of aromaticity. Hence, it is not surprising that they may contradict other indices.

There is a wealth of literature comparing different NICS values to other indices, both from within the magnetic criteria and across criteria of aromaticity. It is infeasible to cover all the studies that show the comparison of NICS to other metrics, and it is outside the scope of this chapter to describe each of these methods in detail. However, to provide the reader with an overview, we have constructed a (non-exhaustive) table that collects representative references of studies that compare NICS-based methods to other methods for evaluating of aromaticity. We have included brief descriptions of the methods and comments on the software needed to perform the different methods, but we refer the reader to the appropriate references for a comprehensive explanation of each method. We also refer the reader to the other chapters of this book, which deal specifically with the evaluation of aromaticity with energetic, geometric and electron-delocalization based methods. For further reading on magnetic criteria for aromaticity evaluation, we refer to our previous review, Reference 3.

Crite rion	Method's Full Name	Acro-nym	Comments on how the values are obtained and/or what they reflect	What software is used?	Relevant citations
	Clar sextets		Counting of Clar sextets. Different resonance structures need to be considered. The resonance structure with the highest number of Clar sextets is expected to be the most contributing one, and NICS values in the corresponding rings are usually the most negative.	Homemade code can enumerate all resonance structures and Clar sextets. There is no commercial program that we know of.	[129,130]
	Y-rule		Extension of Clar rules for polycyclic systems		[131–133]
Energetic	Aromatic Stabilization Energy	ASE	Homodesmotic or isodesmic equations are used to evaluate the stabilization afforded to the molecule due to aromaticity. These can be calculated or based on experimental values. Sometimes artificial reference structures are defined. For isomeric structures, electronic energy differences can be used.	Any quantum chemical program can be used to optimize geometries and obtain the energies of the various components in the equation.	[48,51,51,134]. The reader is also referred to Chapter 6 of this book.
	Pauling-Wheland Resonance energies	RE	This energy is defined as the energy difference between the real, fully conjugated cyclic system and the corresponding virtual most stable resonance structure.	The BLW (Block localized wavefunction) plug-in for GAMESS. Is required in order to calculate the energy of a "frozen" resonance structure.	[135]. The reader is also referred to Chapter 6 of this book.
	Extra cyclic resonance energy	ECRE	ECRE is the difference between the aromatic resonance energies of a fully conjugated cyclic compound and a model with interrupted (acyclic) conjugation. It is designed to consider the stabilization afforded by conjugation, which is disregarded in the Pauling-Wheland resonance energy.	Any quantum chemical program can be used to optimize geometries and obtain the energies of the various components in the equation.	[136]. The reader is also referred to Chapter 6 of this book.
	Hydrogenation energies	$\Delta\Delta H_{H2}$	This method uses the energy released upon hydrogenation of a compound as a measure of its aromaticity. The values can be experimentally obtained or calculated.	Any quantum chemical program can be used to optimize geometries and obtain the energies of the various components in the equation.	[137,138]. The reader is also referred to Chapter 6 of this book.
	Ring deformation energy		The method calculates the conformation flexibility by scanning a relevant torsion angle and uses that energy as a measure of aromatic stabilization. The single report found only shows the application of the method to benzene derivatives.	Any quantum chemical program can be used to optimize geometries and perform scans to obtain the energies of the various components in the equation.	[139]. The reader is also referred to Chapter 6 of this book.

Structural	Harmonic oscillator model of aromaticity	HOMA	The method uses the bond lengths in a conjugated system. It considers two things: how far away are the bond lengths from the ideal bond length (e.g., CC bond length of benzene), and how much bond-length alternation is there. An increase in either/both of these makes the molecule less aromatic. Values range between 0 (not aromatic) and 1 . The new HOMA has been parameterized to allow application to heterocyclic systems, as well. The bond lengths can be calculated or experimental (from crystal structures).	Can be calculated with MultiWFN[140] software. Some authors report using homemade code.	[141–143]. The reader is also referred to Chapter 3 of this book.
	Bond length alternation	BLA	This method is similar to HOMA, but looks only at the bond-length alternation as a measure of aromaticity. The more uniform the bond lengths are, the more aromatic the molecule is considered to be. Values can be computational or experimental. We are not aware of a defined range of values.	No software is known for extraction of geometric data and calculation of BLA.	[144–147]
Magnetic	^{1}H and ^{13}C NMR chemical shifts		Experimental or calculated values are used to evaluate aromaticity, according to the ring current model. Values are isotropic, which can lead to discrepancies with more refined NICS versions.	Any quantum chemical program can be used to optimize geometries and calculate NMR chemical shifts. Values should be calibrated relative to a reference (e.g., $SiMe_4$).	[18,148]
	Anisotropy of the Induced Current	ACID	The ACID scalar field defines the density of delocalized electrons. The isosurface value needs to be chosen by the user. Different values may lead to varying results.	calculated with the ACID plug-in for Gaussian.	17
	Gauge including magnetically induced current	GIMIC	GIMIC shows ring current densities and directions. Based on isotropic values (not only π electrons), so does not necessarily reflect only aromatic currents. Is commonly used for large molecules, such as poly-porphyrin systems.	Implemented in TURBOMOLE[149] and can be plugged in to Gaussian. Plots need to be generated separately, e.g., with JMOL.	[150,151]
	Induced magnetic field, induced magnetic field in the Z direction.	B_Z^{ind}	B_Z^{ind} maps are essentially identical to isosurfaces of $NICS_{ZZ}$ and are often also reported in ppm. They provide a good qualitative (and semi-quantitative) depiction of the induced field in the vicinity of the molecule.	The MIMAF (Molecular Induced Magnetic Fields) program and the Aromagnetic programs are referred to, but could not be located for download.	[152,153]
	Current density analysis	CDA	Current density analysis methods generate plots of arrows, whose size and direction indicate the strength and sense of the ring current. The plots are generated at a certain distance from the molecular plane, so they vary. It is common to use heights of either 1 Å or 1 a_0.	The SYSMOIC program is referenced in multiple publications. The code is available from the authors on request.	[12,154,48,63,38,116]
	Magnetic susceptibility exaltation		This method compares the magnetic susceptibility of an aromatic system to the value that would be expected based on group additivity, thus is requires a reference system. The		[155–157,52]

			values for the group additivity can either be experimentally measured or computationally obtained.		
Electronic	Aromatic fluctuation index	FLU / FLU_{π}	This method uses the atom-in-molecules (AIM) approach to calculate the fluctuation of electronic charge between adjacent atoms, which is used as a measure of aromaticity. The method considers the amount of electron sharing between neighboring atoms as well as the similarity of electron-sharing. Can be applied to rings of any size, and for analysis of both global and local trends Depends on AIM topological analysis.	Can be calculated with the Multiwfn[140] program, which requires a wavefunction files from a quantum-chemical program.	[158]
	Para-delocalization index	PDI	This method measures electron delocalization across the ring. Limited to 6-membered rings. Does not treat heteroatoms with lone-pairs well.	Requires ESI-3D in conjunction with AIM2000/AIMPAC/AIMALL,[159,160] or APOST-3D. Can also be calculated with Multiwfn.[140] These programs require wavefunction or formatted checkpoint files from a quantum-chemical program.	[130,161,162] The reader is also referred to Chapter 7 in this book.
	Electron localization function	ELF	ELF indicates the regions of space that are most probable to find localized electrons. It can be used to study the delocalization of electrons as a measure of aromaticity. Separation of σ and π parts is also possible.	Results have been reported using TopMod[163] or TopChem2 for ELF topological analysis. Visualization with Molekel[164] or SciAn. Multiwfn[140] can also be used.	[165,166,161,167–169]. The reader is also referred to Chapter 7 in this book.
	Bultinck's Multi-center bond index	MCI / MCBI	The multicenter bond index arises from the application of the generalized population analysis to characterize the extent of delocalized cyclic bonding in conjugated cyclic systems. Considers all possible arrangements in the rings (not only Kekuléan). Suffers from size-extensivity problems due to multiplying a number of overlaps.	Homemade code is reported to calculate the overlap matrix using the charge and bond order matrix from the Gaussian formatted checkpoint file (up to 10 centers).	[170,56,171–173]. The reader is also referred to Chapter 7 in this book.
	Giambagi multicenter Index	I_{ring}	This method considers the σ + π electron population in a multicenter bond index for aromaticity evaluation. I_{ring} has been calculated for monocylic systems of varying sizes and for polycylic systems. It takes into account only Kekulé arrangement of the atoms in the ring. As with the MCBI method, it suffers from size-extensivity problems.	Requires ESI-3D in conjunction with AIM2000/AIMPAC/AIMALL,[159,160] or APOST-3D. Can also be calculated with Multiwfn.[140] These programs require wavefunction or formatted checkpoint files from a quantum-chemical program.	[170]. The reader is also referred to Chapter 7 in this book.

	Normalized MCI, I_{ring}.	I_{Nb} , I_{NG}	These are revised versions of the multicenter indices of Bultinck and Giambagi where the *m*th root of the of the index is taken and a normalization factor is added. This has been shows to correlate better with topological resonance energy per electron. These modifications solve the size-extensvity issue.	Requires ESI-3D in conjunction with AIM2000/AIMPAC/AIMALL,[159,160] or APOST-3D. Can also be calculated with Multiwfn.[140] These programs require wavefunction or formatted checkpoint files from a quantum-chemical program.	[174]. The reader is also referred to Chapter 7 in this book.
		AV1245	This method is a multicenter bond that averages the 4-center MCI values along the ring. It is obtained with a different algorithm for calculating multicenter indices, which is specifically designed for large rings. Does not require reference values and is not limited in the type of atoms it can treat or the geometry of the ring. Has been applied also to belt-shaped Möbius structures.	Requires ESI-3D in conjunction with AIM2000/AIMPAC/AIMALL,[159,160] or APOST-3D. Can also be calculated with Multiwfn.[140] These programs require wavefunction or formatted checkpoint files from a quantum-chemical program.	[175]. The reader is also referred to Chapter 7 in this book.
	Electron density of delocalized bonds	EDDB	Probes different levels of electron delocalization by decomposition of the electron density into density layers and identifying those shared between conjugated bonds.	NBO and Gaussian programs are needed, as well as a script prepared by the developers of the method, which is freely available online, along with helpful installation instructions. The script is under active development.	[176]. The reader is also referred to Chapter 8 in this book.

Best Practices for Using NICS

The preceding text describes in detail the limitations and advantages of the various NICS methods. Here, we summarize the "take-home" messages that we wish to provide readers with: a list of "dos and don'ts" to ensure safe use and meaningful interpretation of NICS results.

Single-point vs. multi-point: As a general rule, we recommend using multi-point NICS whenever possible, rather than a single-point calculation. When the values are unambiguous (i.e., easily characterized as aromatic/antiaromatic/nonaromatic), single-point values will provide a safe tool for interpretation. However, when they fall in ranges that are not easily classified (see below), multi-point NICS plots can help determine the character of the system. This is true for both "vertical" NICS-Scans and "horizontal" NICS-*XY*-Scans.

Choice of NICS metric: Of all available NICS metrics, we recommend using $\mathrm{NICS}(1)_{\pi Z}$ at this time. Although the newly developed $\int \mathrm{NICS}_{\pi ZZ}$ is a more refined method, it has only been used for a handful of compounds. Therefore, there are currently not enough data for meaningful comparison, though this may change in the future. Both of these metrics can be calculated with Aroma, which makes them fast and user-friendly.

If limited resources or molecular geometry preclude a $\mathrm{NICS}(1)_{\pi ZZ}$ calculation, we recommend calculating $\mathrm{NICS}(1.7)_{ZZ}$ as a relatively safe alternative. This is especially safe for comparison of systems with similar geometries, in which the contribution of the non-π electrons to the *ZZ* component of the tensor is similar.

We strongly recommend *against* using any of the isotropic methods, namely $\mathrm{NICS}(0)$ and $\mathrm{NICS}(1)$, for characterization of ring currents and aromaticity.

Polycyclic systems: For *cata*- and *peri*-condensed polycyclic systems, the NICS-*XY*-Scan is recommended, using one of the metrics recommended above. If a NICS-*XY*-Scan cannot be calculated, values above the center of each ring should be calculated with one of the recommended metrics. Even if a NICS-*XY*-Scan is not possible, it may be possible to perform a NICS-Scan for the individual rings, which is recommended, especially in cases where values are ambiguous.

Macrocyclic systems: For macrocyclic systems and compounds with geometries that make conventional NICS probe placement difficult, an isosurface of $\mathrm{NICS}(0)$ is currently the most refined description available, but should be interpreted with particular care and results should only be compared to similar systems. If and when possible, $\mathrm{NICS}(0)_{\pi}$ is a better metric for quantitative evaluation of aromaticity.

Dissection methods: One should keep in mind that NICS works best with planar systems, where there is a good separation of π- and σ-orbitals. For planar systems, this dissection can be achieved either with NBO (affording $\mathrm{NICS}(r)_{\pi ZZ}^{\mathrm{CMO}}$ values) or with the σ-Only Model. For non-planar systems, only the σ-Only Model can be applied.

Interpretation of values: Not every negative value indicates aromaticity and not every positive value indicates antiaromaticity. This is especially true for polycyclic systems, where the value in one ring is influenced by effects from neighboring ring. For example, a very strongly antiaromatic ring can generate negative NICS values in neighboring rings, and vice versa. Due to this, from our experience, values in the range -5 < NICS < 5 ppm in polycyclic systems can usually be considered to be nonaromatic. For monocyclic systems, this range can be narrower because NICS values cannot be attributed to neighboring rings: from our experience, we consider -3 < NICS < 3 ppm as nonaromatic. We consider values in the range -15 < NICS

< -5 to be intermediately aromatic, and in the range -25 < NICS < -15 to be strongly aromatic. Note, these ranges are only relevant for $\mathrm{NICS}(1.7)_{\pi ZZ}$.

Benchmarking: It is highly recommended to always compare a calculated value to the respective value for benzene (and/or cyclobutadiene) calculated using the same NICS metric and level of theory. As we showed above, NICS values can change substantially depending on the method used. Such calibration assists immensely in grasping the extent of aromaticity in a studied molecule.

Level of Theory: In general, for structure optimization we recommend using at least triple-zeta basis sets and to include dispersion corrections (note that for small planar system, dispersion is not expected to be very important, but in larger systems CH-π and π-π interactions can become important, e.g., helicenes). For chemical shift calculation, we recommend using a basis set including diffuse functions (e.g., 6-311+G(d) or def2-tzvpd). Though they are not recommended for optimization, our experience has shown that double-zeta basis sets generally provide similar chemical shift results.

NICS in Practice

Having discussed the concept of NICS exhaustively, including its advantages, limitations, and various versions, we believe that it also necessary to demonstrate how it is used—i.e., bring the ideas to realization. Detailed below is one example of a monocyclic system and one of a polycyclic system. We hope this will provide the reader with a good understanding of how the methods are applied and what information is gleaned from them, as well a comparison between the data obtained.

Computational details for the following results: Gaussian 09 was used for all calculations. All systems were fully optimized without any constraints at the B3LYP/6-311G(d) level of theory. All NICS inputs were generated with Aroma, and all NICS output was collected from the Gaussian *.log* file with Aroma, including data for the $\int \mathrm{NICS}$ (scans were done in the 2-5 Å range by changing the range in the *aroma_constants.py* file, the *.armdat* files were read with Excel). All NICS calculations were done at the GIAO-B3LYP/6-311+G(d) // B3LYP/6-311G(d) computational level.

The current density maps were calculated with SYSMOIC at a height of 1 a_0 above the molecular plane. The program allows the user to choose which orbitals will be considered in the calculation. We present results incorporating all orbitals, as well as results stemming only from π-electrons. In the following pages, the following information is shown we present for benzene:

a. Figure showing the placement of the NICS probes for a vertical NICS-Scan. Probes are depicted in pink.
b. Figure showing the placement of the NICS probes for a vertical NICS-Scan on a σ-Only Model of the system. Note that the probes are placed on the face opposite the model's hydrogens.
c. The Aroma input file (*.arm*) for running NICS analyses on the compound using the Aroma utility for Gaussian. The coordinate for starting the NICS-Scan is chosen to be at the center of the cycle by specifying the numbers of the corresponding atoms, according to their sequence in the geometry input file. The charge of the σ-Only Model can also be specified; for benzene it is neutral, but for a heterocycle, such as furan, the model will have a +1 charge and for a trivalent atom (e.g., boron), the charge will be -1.

d. An excerpt from an Aroma-generated output file for a CMO-NICS analysis (*.picmo*). The first three NICS probes are shown, corresponding to the height 0—0.2 Å from the molecular plane. Aroma identifies the π-MOs (in the benzene example, these are MOs 17, 20, and 21), and calculates the negative of the sum of these contributions at each distance point.
e. An excerpt from the Gaussian output (*.log*) file detailing the chemical shift tensor calculation. The first two NICS probes are shown (corresponding to heights 0 and 0.1 Å from the molecular plane).
f. An excerpt from an Aroma-generated output file for a NICS-Scan analysis (*.armdat*). The first three NICS probes are shown, corresponding to the height 0–0.2 Å from the molecular plane. The “oop” and “z” columns correspond to the out-of-plane component and the ZZ component of the chemical shift tensor. Note that the first two values in the “z” column are identical to the negative of the ZZ component in panel e. For a σ-Only Model analysis, the same type of file will be generated for the model system.
g. Plots of $3\Delta_{\mathrm{iso}}$, $\mathrm{NICS}_{\pi ZZ}^{\mathrm{CMO}}$, and $\mathrm{NICS}_{\pi ZZ}^{\mathrm{SOM}}$ for the heights 1—4 Å. These plots are generated from the data seen in the excerpts in the panels d and f, starting from the NICS probe at the height 1 Å. To generate the $3\Delta_{\mathrm{iso}}$ and $\mathrm{NICS}_{\pi ZZ}^{\mathrm{SOM}}$, Aroma subtracts the data of the model system from the delocalized one.
h. An excerpt from an Aroma-generated summary output file (*.armlog*), which details the fitting functions obtained from the plots seen in panel g.
i. Plots of $3\Delta_{\mathrm{iso}}$, $\mathrm{NICS}_{\pi ZZ}^{\mathrm{CMO}}$, and $\mathrm{NICS}_{\pi ZZ}^{\mathrm{SOM}}$ for the heights 2—5 Å. These plots are generated from the file such as the ones seen panels d and f, but for the modified height range. To generate the $3\Delta_{\mathrm{iso}}$ and $\mathrm{NICS}_{\pi ZZ}^{\mathrm{SOM}}$, Aroma subtracts the data of the model system from the delocalized one.
j. Excerpt from an Excel sheet used for fitting the data in the height range 2—5 Å to obtain $\int \mathrm{NICS}$.
k. Current density maps calculated for the studied compound considering all electrons (left) and considering only the π-electrons (right)

Preprint of Chapter 4 in the book “Aromaticity: Modern Computational Methods and Applications”
Ed. Israel Fernandez, Pub. Elsevier, May 2021

a)

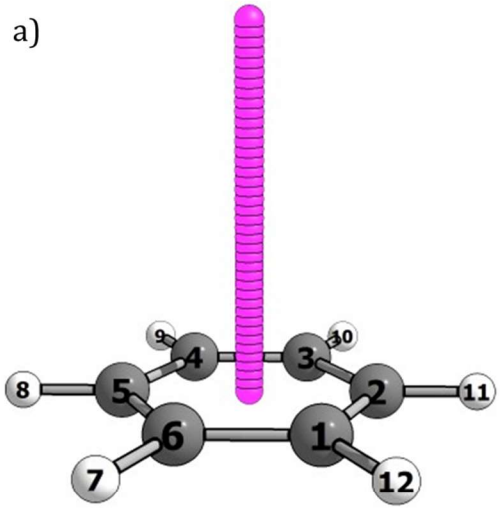

b)

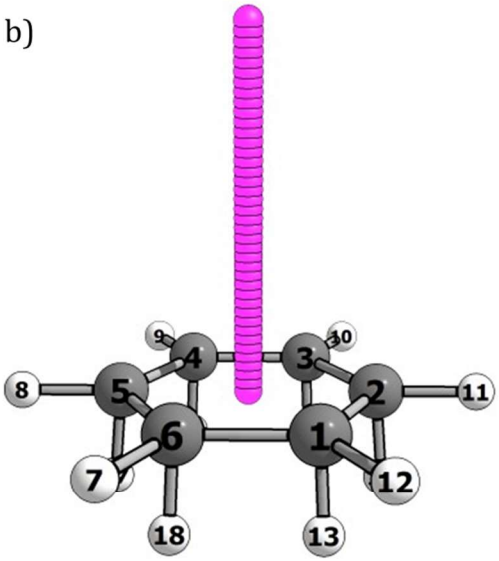

c)

```
geomfile=<path to geometry file>
run=nicsscan,sigma
center=1,2,3,4,5,6
aromatic ring
1,2,3,4,5,6
end
sonly charge = 0
```

d)

pi-MO#	17	20	21	-Sum
0.00	12.74	11.55	11.55	-35.84
0.10	12.76	11.54	11.53	-35.83
0.20	12.80	11.49	11.48	-35.77

e)

```
  13  Bq   Isotropic =     7.9106   Anisotropy =     9.4059
XX=     4.7738   YX=     0.0001   ZX=     0.0000
XY=     0.0012   YY=     4.7768   ZY=     0.0001
XZ=     0.0000   YZ=     0.0000   ZZ=    14.1812
Eigenvalues:     4.7737     4.7769    14.1812
  14  Bq   Isotropic =     8.0168   Anisotropy =     9.9398
XX=     4.7021   YX=     0.0001   ZX=     0.0000
XY=     0.0012   YY=     4.7051   ZY=     0.0001
XZ=     0.0000   YZ=     0.0000   ZZ=    14.6433
Eigenvalues:     4.7019     4.7052    14.6433
```

f)

#	oop	in1	in2	inp	iso	x	y	z
0.00	-14.1812	-4.7769	-4.7737	-4.7753	-7.9106	-4.7738	-4.7768	-14.1812
0.10	-14.6433	-4.7052	-4.7019	-4.7036	-8.0168	-4.7021	-4.7051	-14.6433
0.20	-15.9587	-4.4957	-4.4924	-4.4941	-8.3156	-4.4925	-4.4955	-15.9587

g)

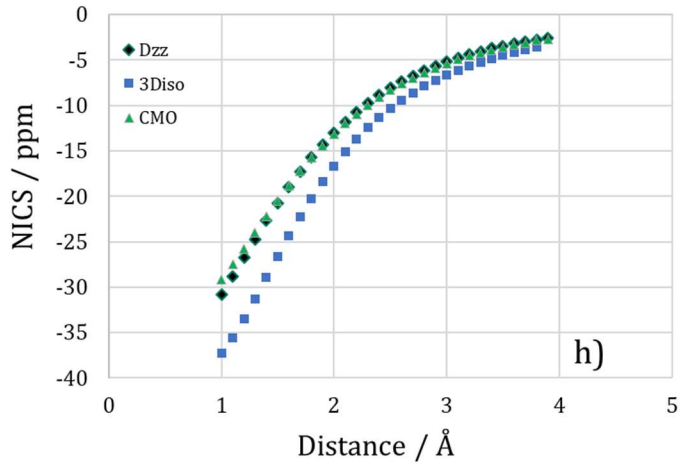

h)

```
------------------------------------------------------------
                    ** Aroma Run **
------------------------------------------------------------


For Center 1
------------------------------------------------------------
Polynomials for Doop and 3Diso are :

         3          2
0.7773 x - 9.696 x + 41.73 x - 64.03
         3          2
0.5331 x - 8.679 x + 43.78 x - 74.08

The mean NICS value is -34.832 with error 3.615
------------------------------------------------------------
```

i)

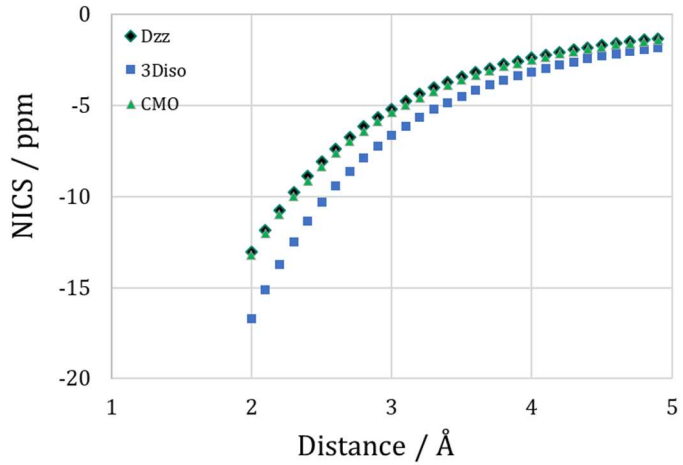

j)

benzene for ∫NICS	ZZ	3Δiso	σ-only π	±	CMO
A	-70.77	-86.97			-68.96
B	0.42	0.43			0.43
∫NICS=A*B^∞/lan(B)-A/lan(B)	-82.27	-103.14	-92.71	10.44	-82.18

k)

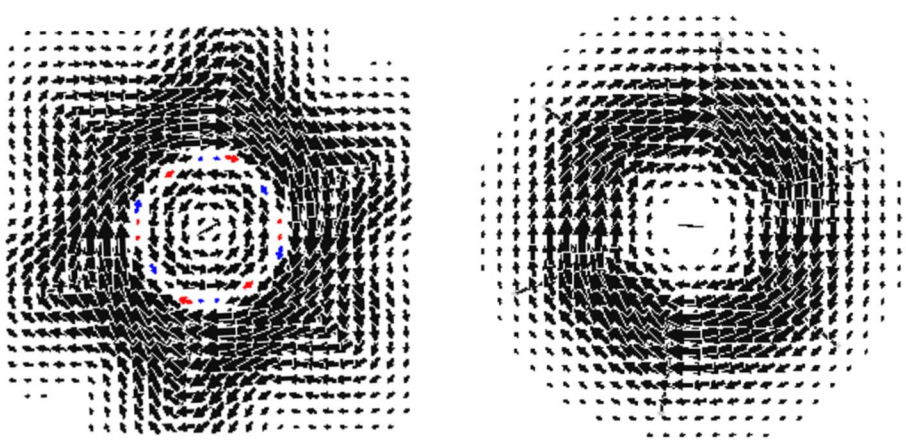

Polycyclic system – Anthracene

In the following pages, we present the following information for anthracene:

a. Figure showing the placement of the NICS probes for a NICS-*XY*-Scan at a height of 1.7 Å. Probes are indicated in pink
b. Figure showing the placement of the NICS probes for a NICS-*XY*-Scan on a σ-Only Model of the system at a height of 1.7 Å opposite the model’s hydrogens.
c. The Aroma input file (*.arm*) for running a NICS-*XY*-Scan on the compound using the Aroma utility for Gaussian. The pathway the *XY*-scan is defined by indicating the centers of the rings and bonds that the path should go through. The centers are given by the corresponding numbers of the atoms, according to their order of appearance in the geometry input file. The charge of the σ-Only Model can also be specified; for anthracene it is neutral, but for a systems containing heterocycles, the model may have a positive or negative charge.
d. An excerpt from an Aroma-generated output file for a NICS-Scan analysis (*alldiff.armlog*). The first six NICS probes are shown, corresponding to the distance 0—0.5 Å of the scan path. The “ZZ” and “Sigma-ZZ” columns correspond to the *ZZ* component of the chemical shift tensor for the delocalized system and the σ-Only Model, respectively. The “Del-ZZ” column is the difference between them, i.e., $\mathrm{NICS}_{\pi ZZ}^{\mathrm{SOM}}$.
e. An excerpt from an Aroma-generated output file for a CMO-NICS analysis (*.picmo*). The first six NICS probes are shown, corresponding to the distance 0—0.5 Å of the scan path. Aroma identifies the π-MOs (for the anthracene example these are MOs 36, 39, 43, 44, 45, 46, and 47), and calculates the negative of the sum of these contributions at each distance point.
f. Plots of $NICS_{ZZ}$, $NICS_{\pi ZZ}^{CMO}$ and $NICS_{\pi ZZ}^{SOM}$. These are the plots generated from the data seen in the excerpts in the panels d and e.
g. An excerpt from an Aroma-generated output file for a NICS-*XY*-Scan (*.armlog*), specifying the coordinates determining the pathway of the scan. The coordinates correspond to the centers defined by the input file (panel c) and allow the user to identify the exact location of the respective points along the pathway.
h. Current density maps calculated for the studied compound considering all electrons (left) and considering only the π-electrons (right). These plots highlight the importance of dissection of the NICS values.

Preprint of Chapter 4 in the book “Aromaticity: Modern Computational Methods and Applications”
Ed. Israel Fernandez, Pub. Elsevier, May 2021

Anthracene

a)

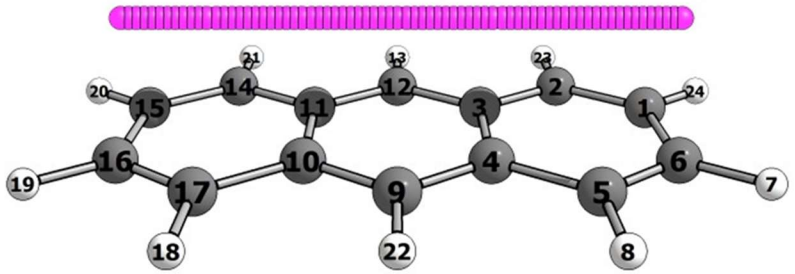

b)

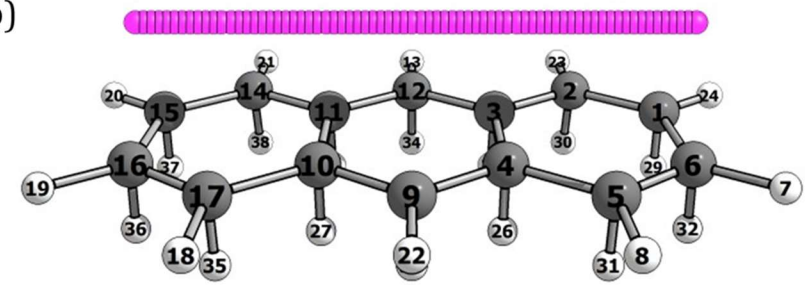

c)

```
geomfile=<path to geometry file>
run=xy,nicsscan,sigma
center=1,6
center=1,2,3,4,5,6
center=3,4
center=3,4,9,10,11,12
center=10,11
center=10,11,14,15,16,17
center=13,14
aromatic ring
1,2,3,4,5,6
3,4,9,10,11,12
10,11,14,15,16,17
end
sonly charge = 0
```

d)

r	ZZ	Sigma-ZZ	Del-ZZ
0.00	-15.2779	-5.6192	-9.6587
0.10	-16.4498	-5.6318	-10.8180
0.20	-17.4703	-5.5511	-11.9192
0.30	-18.3258	-5.3921	-12.9337
0.40	-19.0147	-5.1751	-13.8396
0.50	-19.5459	-4.9233	-14.6226

e)

pi-MO #	36	39	43	44	45	46	47	-Sum
0.00	2.80	2.92	3.22	-1.18	-0.01	2.10	0.10	-9.95
0.10	2.96	3.17	3.48	-1.19	-0.03	2.55	0.14	-11.08
0.20	3.13	3.42	3.72	-1.20	-0.05	2.96	0.18	-12.16
0.30	3.30	3.64	3.91	-1.21	-0.06	3.30	0.21	-13.09
0.40	3.48	3.85	4.07	-1.23	-0.07	3.58	0.25	-13.93
0.50	3.65	4.03	4.20	-1.24	-0.08	3.79	0.27	-14.62

f)

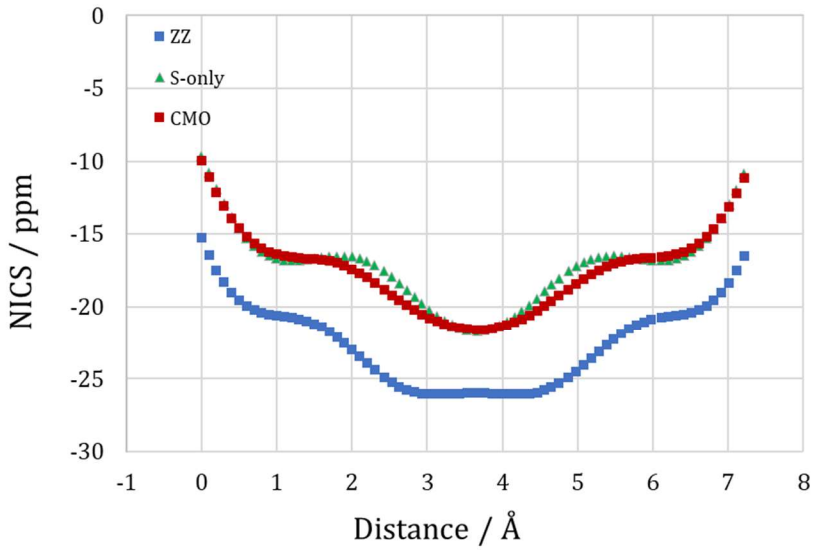

g)

```
------------------------------------------------------------------
                    ** Aroma Run **
------------------------------------------------------------------

For the Original Molecule:


The Centers for Rings/Bonds from the .arm file corresponds to following BQs
Ring  Distance     X        Y        Z
  1      0.0    1.204    0.000    1.700
  2      1.2   -0.000    0.000    1.700
  3      2.4   -1.229    0.000    1.700
  4      3.7   -2.451    0.000    1.700
  5      4.9   -3.673    0.000    1.700
  6      6.1   -4.903    0.000    1.700
  7      7.3   -6.107    0.000    1.700

------------------------------------------------------------------
```

h)

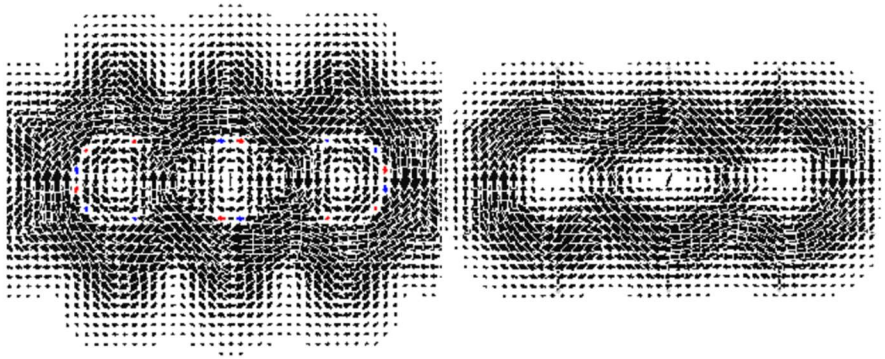

(1) Schleyer, P. v R.; Maerker, C.; Dransfeld, A.; Jiao, H.; van Eikema Hommes, N. J. R. Nucleus-Independent Chemical Shifts: A Simple and Efficient Aromaticity Probe. *J. Am. Chem. Soc.* **1996**, *118* (26), 6317–6318.
(2) Chen, Z.; Wannere, C. S.; Corminboeuf, C.; Puchta, R.; Schleyer, P. von R. Nucleus-Independent Chemical Shifts (NICS) as an Aromaticity Criterion. *Chem. Rev. (Washington, DC, U. S.)* **2005**, *105* (10), 3842–3888.
(3) Gershoni-Poranne, R.; Stanger, A. Magnetic Criteria of Aromaticity. *Chem. Soc. Rev.* **2015**, *44* (18), 6597–6615.
(4) Stanger, A. NICS – Past and Present. *Eur. J. Org. Chem.* **2020**, 3120–3127.
(5) McWeeny, R. Ring Currents and Proton Magnetic Resonance in Aromatic Molecules. *Mol. Phys.* **1958**, *1* (4), 311–321.
(6) Pople, J. A. Molecular Orbital Theory of Aromatic Ring Currents. *Mol. Phys.* **1958**, *1* (2), 175–180.
(7) London, F. Théorie Quantique Des Courants Interatomiques Dans Les Combinaisons Aromatiques. *J. Phys. Radium* **1937**, *8* (10), 397–409.
(8) Huckel theory for organic chemists / C. A. Coulson, Brian O’Leary, and R. B. Mallion | National Library of Australia https://catalogue.nla.gov.au/Record/2555212 (accessed Jun 11, 2020).
(9) Dickens, T. K.; Mallion, R. B. Topological Ring-Currents in Conjugated Systems. *MATCH Commun. Math. Comput. Chem.* **2016**, *76*, 297–356.
(10) Monaco, G.; Zanasi, R. Assessment of Ring Current Models for Monocycles. *J. Phys. Chem. A* **2014**, *118* (9), 1673–1683.
(11) Fowler, P. W.; Steiner, E. Pseudo-π Currents: Rapid and Accurate Visualisation of Ring Currents in Conjugated Hydrocarbons. *Chem. Phys. Lett.* **2002**, *364* (3,4), 259–266.
(12) Fowler, P. W.; Steiner, E.; Havenith, R. W. A.; Jenneskens, L. W. Current Density, Chemical Shifts and Aromaticity. *Magn. Reson. Chem.* **2004**, *42* (Spec. Issue), S68–S78.
(13) Steiner, E.; Fowler, P. W. Patterns of Ring Currents in Conjugated Molecules: A Few-Electron Model Based on Orbital Contributions. *J. Phys. Chem. A* **2001**, *105* (41), 9553–9562.
(14) Steiner, E.; Fowler, P. W. Four- and Two-Electron Rules for Diatropic and Paratropic Ring Currents in Monocyclic Ï€ Systems. *Chemical Communications* **2001**, No. 21, 2220–2221.
(15) Pérez-Juste, I.; Mandado, M.; Carballeira, L. Contributions from Orbital–Orbital Interactions to Nucleus-Independent Chemical Shifts and Their Relation with Aromaticity or Antiaromaticity of Conjugated Molecules. *Chemical Physics Letters* **2010**, *491* (4), 224–229.
(16) Fliegl, H.; Taubert, S.; Lehtonen, O.; Sundholm, D. The Gauge Including Magnetically Induced Current Method. *Phys. Chem. Chem. Phys.* **2011**, *13* (46), 20500–20518.
(17) Geuenich, D.; Hess, K.; Köhler, F.; Herges, R. Anisotropy of the Induced Current Density (ACID), a General Method To Quantify and Visualize Electronic Delocalization. *Chem. Rev.* **2005**, *105* (10), 3758–3772.
(18) Mitchell, R. H. Measuring Aromaticity by NMR. *Chem. Rev. (Washington, D. C.)* **2001**, *101* (5), 1301–1315.
(19) Faglioni, F.; Ligabue, A.; Pelloni, S.; Soncini, A.; Viglione, R. G.; Ferraro, M. B.; Zanasi, R.; Lazzeretti, P. Why Downfield Proton Chemical Shifts Are Not Reliable Aromaticity Indicators. *Org. Lett.* **2005**, *7* (16), 3457–3460.
(20) Fowler, P. W.; Lazzeretti, P.; Zanasi, R. Electric and Magnetic Properties of the Aromatic Sixty-Carbon Cage. *Chemical Physics Letters* **1990**, *165* (1), 79–86.
(21) Zanasi, R.; Fowler, P. W. Ring Currents and Magnetisability in C60. *Chemical Physics Letters* **1995**, *238* (4), 270–280.
(22) Buhl, M. The Relation between Endohedral Chemical Shifts and Local Aromaticities in Fullerenes. *Chem. - Eur. J.* **1998**, *4* (4), 734–739.

(23) Schleyer, P. von R.; Jiao, H.; van Eikema Hommes, N. J. R.; Malkin, V. G.; Malkina, O. An Evaluation of the Aromaticity of Inorganic Rings: Refined Evidence from Magnetic Properties. *J. Am. Chem. Soc.* **1997**, *119* (51), 12669–12670.

(24) Schleyer, P. von R.; Manoharan, M.; Wang, Z.-X.; Kiran, B.; Jiao, H.; Puchta, R.; van Eikema Hommes, N. J. R. Dissected Nucleus-Independent Chemical Shift Analysis of π-Aromaticity and Antiaromaticity. *Org. Lett.* **//**, *3* (16), 2465–2468.

(25) Fowler, P. W.; Steiner, E.; Zanasi, R.; Cadioli, B. Electric and Magnetic Properties of Hexaethynylbenzene. *Mol. Phys.* **1999**, *96* (7), 1099–1108.

(26) Steiner, E.; Fowler, P. W.; Jenneskens, L. W. Counter-Rotating Ring Currents in Coronene and Corannulene. *Angew. Chem., Int. Ed.* **2001**, *40* (2), 362–366.

(27) Corminboeuf, C.; Heine, T.; Weber, J. Evaluation of Aromaticity: A New Dissected NICS Model Based on Canonical Orbitals. *Phys. Chem. Chem. Phys.* **2007**, *5* (2), 246–251.

(28) Foroutan-Nejad, C.; Shahbazian, S.; Feixas, F.; Rashidi-Ranjbar, P.; Solà, M. A Dissected Ring Current Model for Assessing Magnetic Aromaticity: A General Approach for Both Organic and Inorganic Rings. *J. Comput. Chem.* **2011**, *32* (11), 2422–2431.

(29) Heine, T.; Schleyer, P. v. R.; Corminboeuf, C.; Seifert, G.; Reviakine, R.; Weber, J. Analysis of Aromatic Delocalization: Individual Molecular Orbital Contributions to Nucleus-Independent Chemical Shifts. *J. Phys. Chem. A* **2003**, *107* (33), 6470–6475.

(30) Bohmann, J. A.; Weinhold, F.; Farrar, T. C. Natural Chemical Shielding Analysis of Nuclear Magnetic Resonance Shielding Tensors from Gauge-Including Atomic Orbital Calculations. *J. Chem. Phys.* **1997**, *107* (4), 1173–1184.

(31) Glendening, E. D.; Landis, C. R.; Weinhold, F. Natural Bond Orbital Methods. *WIREs Computational Molecular Science* **2012**, *2* (1), 1–42.

(32) Frisch, M. J.; Trucks, G. W.; Schlegel, H. B.; Scuseria, G. E.; Robb, M. A.; Cheeseman, J. R.; Scalmani, G.; Barone, V.; Mennucci, B.; Petersson, G. A.; Nakatsuji, H.; Caricato, M.; Li, X.; Hratchian, H. P.; Izmaylov, A. F.; Bloino, J.; Zheng, G.; Sonnenberg, J. L.; Hada, M.; Ehara, M.; Toyota, K.; Fukuda, R.; Hasegawa, J.; Ishida, M.; Nakajima, T.; Honda, Y.; Kitao, O.; Nakai, H.; Vreven, T.; Montgomery, J. A.; Peralta, J. E.; Ogliaro, F.; Bearpark, M.; Heyd, J. J.; Brothers, E.; Kudin, K. N.; Staroverov, V. N.; Kobayashi, R.; Normand, J.; Raghavachari, K.; Rendell, A.; Burant, J. C.; Iyengar, S. S.; Tomasi, J.; Cossi, M.; Rega, N.; Millam, J. M.; Klene, M.; Knox, J. E.; Cross, J. B.; Bakken, V.; Adamo, C.; Jaramillo, J.; Gomperts, R.; Stratmann, R. E.; Yazyev, O.; Austin, A. J.; Cammi, R.; Pomelli, C.; Ochterski, J. W.; Martin, R. L.; Morokuma, K.; Zakrzewski, V. G.; Voth, G. A.; Salvador, P.; Dannenberg, J. J.; Dapprich, S.; Daniels, A. D.; Farkas; Foresman, J. B.; Ortiz, J. V.; Cioslowski, J.; Fox, D. J. Gaussian 09, Revision B.01. *Gaussian 09, Revision B.01, Gaussian, Inc., Wallingford CT* **2009**.

(33) Neese, F. The ORCA Program System. *WIREs Comp. Mol. Sci.* **2012**, *2* (1), 73–78.

(34) Neese, F. Software Update: The ORCA Program System, Version 4.0. *WIREs Comp. Mol. Sci.* **2018**, *8* (1), e1327.

(35) Dobrowolski, J. C.; Lipinski, P. F. J. On Splitting of the NICS(1) Magnetic Aromaticity Index. *RSC Adv.* **//**, *6* (28), 23900–23904.

(36) Stanger, A. Obtaining Relative Induced Ring Currents Quantitatively from NICS. *J. Org. Chem.* **2010**, *75* (7), 2281–2288.

(37) Fallah-Bagher-Shaidaei, H.; Wannere, C. S.; Corminboeuf, C.; Puchta, R.; Schleyer, P. v R. Which NICS Aromaticity Index for Planar π Rings Is Best? *Org. Lett.* **2006**, *8* (5), 863–866.

(38) Báez-Grez, R.; Ruiz, L.; Pino-Rios, R.; Tiznado, W. Which NICS Method Is Most Consistent with Ring Current Analysis? Assessment in Simple Monocycles. *RSC Adv.* **2018**, *8* (24), 13446–13453.

(39) Van Damme, S.; Acke, G.; Havenith, R. W. A.; Bultinck, P. Can the Current Density Map Topology Be Extracted from the Nucleus Independent Chemical Shifts? *Phys. Chem. Chem. Phys.* **2016**, *18* (17), 11746–11755.

(40) Nyulászi, L.; Schleyer, P. von R. Hyperconjugative π-Aromaticity: How To Make Cyclopentadiene Aromatic. *J. Am. Chem. Soc.* **1999**, *121* (29), 6872–6875.
(41) Stanger, A. Can Substituted Cyclopentadiene Become Aromatic or Antiaromatic? *Chem. - Eur. J.* **2006**, *12* (10), 2745–2751.
(42) Islas, R.; Martínez-Guajardo, G.; Jiménez-Halla, J. O. C.; Solà, M.; Merino, G. Not All That Has a Negative NICS Is Aromatic: The Case of the H-Bonded Cyclic Trimer of HF. *J. Chem. Theory Comput.* **2010**, *6* (4), 1131–1135.
(43) Juselius, J.; Sundholm, D. Ab Initio Determination of the Induced Ring Current in Aromatic Molecules. *Phys. Chem. Chem. Phys.* **1999**, *1* (15), 3429–3435.
(44) Jusélius, J.; Sundholm, D. The Aromaticity and Antiaromaticity of Dehydroannulenes. *Physical Chemistry Chemical Physics* **2001**, *3* (12), 2433–2437.
(45) Klod, S.; Kleinpeter, E. Ab Initio Calculation of the Anisotropy Effect of Multiple Bonds and the Ring Current Effect of Arenes—Application in Conformational and Configurational Analysis. *J. Chem. Soc., Perkin Trans. 2* **2001**, No. 10, 1893–1898.
(46) Kleinpeter, E.; Klod, S.; Koch, A. Visualization of through Space NMR Shieldings of Aromatic and Anti-Aromatic Molecules and a Simple Means to Compare and Estimate Aromaticity. *J. Mol. Struct.: THEOCHEM* **2007**, *811* (1–3), 45–60.
(47) Stanger, A. Nucleus-Independent Chemical Shifts (NICS): Distance Dependence and Revised Criteria for Aromaticity and Antiaromaticity. *J. Org. Chem.* **2006**, *71* (3), 883–893.
(48) Gershoni-Poranne, R.; Gibson, C. M.; Fowler, P. W.; Stanger, A. Concurrence between Current Density, Nucleus-Independent Chemical Shifts, and Aromatic Stabilization Energy: The Case of Isomeric 4 - and 5 Phenylenes. *J. Org. Chem.* **2013**, *78* (15), 7544–7553.
(49) Gershoni-Poranne, R.; Rahalkar, A. P.; Stanger, A. The Predictive Power of Aromaticity: Quantitative Correlation between Aromaticity and Ionization Potentials and HOMO–LUMO Gaps in Oligomers of Benzene, Pyrrole, Furan, and Thiophene. *Phys. Chem. Chem. Phys.* **2018**, *20* (21), 14808–14817.
(50) Stanger, A. Reexamination of NICSπ,Zz: Height Dependence, Off-Center Values, and Integration. *J. Phys. Chem. A* **2019**, *123* (17), 3922–3927.
(51) Stanger, A. Aromatic Stabilization Energy and Magnetic Properties in Fulvalenes: Is There a Connection Between These Two Aromaticity Indices? *J. Org. Chem.* **2013**, *78* (24), 12374–12380.
(52) Mills, N. S.; Llagostera, K. B. Summation of Nucleus Independent Chemical Shifts as a Measure of Aromaticity. *J. Org. Chem.* **2007**, *72* (24), 9163–9169.
(53) Alvarez-Ramírez, F.; Ruiz-Morales, Y. Database of Nuclear Independent Chemical Shifts (NICS) versus NICSZZ of Polycyclic Aromatic Hydrocarbons (PAHs). *J. Chem. Inf. Model.* **2019**.
(54) Bultinck, P. Critical Analysis of the Local Aromaticity Concept in Polyaromatic Hydrocarbons. *Faraday Discussions* **2007**, *135* (0), 347–365.
(55) Fowler, P. W.; Myrvold, W. The "Anthracene Problem": Closed-Form Conjugated-Circuit Models of Ring Currents in Linear Polyacenes. *J. Phys. Chem. A* **2011**, *115* (45), 13191–13200.
(56) Bultinck, P.; Rafat, M.; Ponec, R.; Van Gheluwe, B.; Carbo-Dorca, R.; Popelier, P. Electron Delocalization and Aromaticity in Linear Polyacenes: Atoms in Molecules Multicenter Delocalization Index. *J. Phys. Chem. A* **2006**, *110* (24), 7642–7648.
(57) Kaipio, M.; Patzschke, M.; Fliegl, H.; Pichierri, F.; Sundholm, D. Effect of Fluorine Substitution on the Aromaticity of Polycyclic Hydrocarbons. *J. Phys. Chem. A* **2012**, *116* (41), 10257–10268.
(58) Aihara, J.; Kanno, H. Local Aromaticities in Large Polyacene Molecules. *J. Phys. Chem. A* **2005**, *109* (16), 3717–3721.
(59) Aihara, J.; Ishida, T.; Kanno, H. Bond Resonance Energy as an Indicator of Local Aromaticity. *Bull. Chem. Soc. Jpn.* **2007**, *80* (8), 1518–1521.

(60) Portella, G.; Poater, J.; Bofill, J. M.; Alemany, P.; Sola, M. Local Aromaticity of [n]Acenes, [n]Phenacenes, and [n]Helicenes (n = 1-9). *J. Org. Chem.* **2005**, *70* (7), 2509–2521.
(61) Bultinck, P.; Fias, S.; Ponec, R. Local Aromaticity in Polycyclic Aromatic Hydrocarbons: Electron Delocalization versus Magnetic Indices. *Chem. - Eur. J.* **2006**, *12* (34), 8813–8818.
(62) Gershoni-Poranne, R.; Stanger, A. The NICS-XY-Scan: Identification of Local and Global Ring Currents in Multi- Ring Systems. *Chem. - Eur. J.* **2014**, *20* (19), 5673–5688.
(63) Stanger, A.; Monaco, G.; Zanasi, R. NICS-XY-Scan Predictions of Local, Semi-Global, and Global Ring Currents in Annulated Pentalene and s-Indacene Cores Compared to First-Principles Current Density Maps. *ChemPhysChem n/a* (n/a).
(64) Gershoni-Poranne, R. Piecing It Together: An Additivity Scheme for Aromaticity Using NICS-XY-Scans. *Chemistry – A European Journal* **2018**, 4165–4172.
(65) Finkelstein, P.; Gershoni-Poranne, R. An Additivity Scheme for Aromaticity: The Heteroatom Case. *ChemPhysChem* **2019**, *20*, 1508–1520.
(66) Liu, C.; Ni, Y.; Lu, X.; Li, G.; Wu, J. Global Aromaticity in Macrocyclic Polyradicaloids: Hückel's Rule or Baird's Rule? *Acc. Chem. Res.* **2019**, *52* (8), 2309–2321.
(67) Ni, Y.; Gopalakrishna, T. Y.; Phan, H.; Kim, T.; Herng, T. S.; Han, Y.; Tao, T.; Ding, J.; Kim, D.; Wu, J. 3D Global Aromaticity in a Fully Conjugated Diradicaloid Cage at Different Oxidation States. *Nat. Chem.* **2020**, *12* (3), 242–248.
(68) Lu, X.; Gopalakrishna, T. Y.; Phan, H.; Herng, T. S.; Jiang, Q.; Liu, C.; Li, G.; Ding, J.; Wu, J. Global Aromaticity in Macrocyclic Cyclopenta-Fused Tetraphenanthrenylene Tetraradicaloid and Its Charged Species. *Angew. Chem., Int. Ed.* **2018**, *57* (40), 13052–13056.
(69) Peeks, M. D.; Claridge, T. D. W.; Anderson, H. L. Aromatic and Antiaromatic Ring Currents in a Molecular Nanoring. *Nature (London, U. K.)* **2017**, *541* (7636), 200–203.
(70) Peeks, M.; Gong, J.; McLoughlin, K.; Kobatake, T.; Haver, R.; Herz, L.; Anderson, H. L. Aromaticity and Antiaromaticity in the Excited States of Porphyrin Nanorings.
(71) Rickhaus, M.; Jirasek, M.; Tejerina, L.; Gotfredsen, H.; Peeks, M. D.; Haver, R.; Jiang, H.-W.; Claridge, T. D. W.; Anderson, H. L. Global Aromaticity at the Nanoscale. *Nat. Chem.* **2020**, *12* (3), 236–241.
(72) Peeks, M. D.; Jirasek, M.; Claridge, T. D. W.; Anderson, H. L. Global Aromaticity and Antiaromaticity in Porphyrin Nanoring Anions. *Angew. Chem., Int. Ed.* **2019**, *58* (44), 15717–15720.
(73) Monajjemi, M.; Mohammadian, N. T. S-NICS: An Aromaticity Criterion for Nano Molecules. *J. Comput. Theor. Nanosci.* **2015**, *12* (11), 4895–4914.
(74) Williams, R. V. Homoaromaticity. *Chem. Rev.* **2001**, *101* (5), 1185–1204.
(75) Aihara, J. Is Superaromaticity a Fact or an Artifact? The Kekulene Problem. *J. Am. Chem. Soc.* **1992**, *114* (3), 865–868.
(76) Soncini, A.; W. Fowler, P.; Lepetit, C.; Chauvin, R. Aromaticity of Ring Carbo-Mers of [N]Annulenes and [N]Cycloalkanes. *Phys. Chem. Chem. Phys.* **2008**, *10* (7), 957–964.
(77) Cocq, K.; Lepetit, C.; Maraval, V.; Chauvin, R. "Carbo-Aromaticity" and Novel Carbo-Aromatic Compounds. *Chem. Soc. Rev.* **2015**, *44* (18), 6535–6559.
(78) Feixas, F.; Matito, E.; Poater, J.; Solà, M. Metalloaromaticity. *WIREs Comp. Mol. Sci.* **2013**, *3* (2), 105–122.
(79) Chamizo, J. A.; Morgado, J.; Sosa, P. Organometallic Aromaticity. *Organometallics* **1993**, *12* (12), 5005–5007.
(80) Chen, D.; Xie, Q.; Zhu, J. Unconventional Aromaticity in Organometallics: The Power of Transition Metals. *Acc. Chem. Res.* **2019**, *52* (5), 1449–1460.
(81) Levandowski, B. J.; Zou, L.; Houk, K. N. Schleyer Hyperconjugative Aromaticity and Diels-Alder Reactivity of 5-Substituted Cyclopentadienes. *J. Comput. Chem.* **2016**, *37* (Copyright (C) 2018 American Chemical Society (ACS). All Rights Reserved.), 117–123.

(82) Levandowski, B. J.; Zou, L.; Houk, K. N. Hyperconjugative Aromaticity and Antiaromaticity Control the Reactivities and π-Facial Stereoselectivities of 5-Substituted Cyclopentadiene Diels–Alder Cycloadditions. *J. Org. Chem.* **2018**, *83* (23), 14658–14666.

(83) Xie, Q.; Sun, T.; Orozco-Ic, M.; Barroso, J.; Zhao, Y.; Merino, G.; Zhu, J. Probing Hyperconjugative Aromaticity of Monosubstituted Cyclopentadienes. *Asian Journal of Organic Chemistry* **2019**, *8* (1), 123–127.

(84) Fernandez, I.; Wu, J. I.; Schleyer, P. von Rague. Substituent Effects on "Hyperconjugative" Aromaticity and Antiaromaticity in Planar Cyclopolyenes. *Org. Lett.* **2013**, *15* (Copyright (C) 2018 American Chemical Society (ACS). All Rights Reserved.), 2990–2993.

(85) Alonso, M.; Herradón, B. Substituent Effects on the Aromaticity of Carbocyclic Five-Membered Rings. *Phys. Chem. Chem. Phys.* **2010**, *12* (6), 1305–1317.

(86) Cioslowski, J.; O'Connor, P. B.; Fleischmann, E. D. Is Superbenzene Superaromatic? *J. Am. Chem. Soc.* **1991**, *113* (4), 1086–1089.

(87) Jiao, H.; Schleyer, P. von R. Is Kekulene Really Superaromatic? *Angew. Chem., Int. Ed.* **1996**, *35* (20), 2383–2386.

(88) Aihara, J. Nucleus-Independent Chemical Shifts and Local Aromaticities in Large Polycyclic Aromatic Hydrocarbons. *Chem. Phys. Lett.* **2002**, *365* (1,2), 34–39.

(89) Aihara, J.; Makino, M.; Ishida, T.; Dias, J. R. Analytical Study of Superaromaticity in Cycloarenes and Related Coronoid Hydrocarbons. *J. Phys. Chem. A* **2013**, *117* (22), 4688–4697.

(90) Yoshida, M.; Ōsawa, E.; Aihara, J. Aromaticity and Superaromaticity in Carbon Nanotoroids. *J. Chem. Soc. Faraday Trans.* **1995**, *91* (11), 1563–1565.

(91) Monaco, G.; Scott, E. L. T.; Zanasi, R. Reversal of Clar's Aromatic-Sextet Rule in Ultrashort Single-End-Capped [5,5] Carbon Nanotubes. *ChemistryOpen* **2020**, *9* (5), 616–622.

(92) Popov, I. A.; Boldyrev, A. I. Chemical Bonding in Inorganic Aromatic Compounds. In *The Chemical Bond*; John Wiley & Sons, Ltd, 2014; pp 421–444.

(93) Baldridge, K. K.; Uzan, O.; Martin, J. M. L. The Silabenzenes: Structure, Properties, and Aromaticity. *Organometallics* **2000**, *19* (8), 1477–1487.

(94) Subramanian, G.; Schleyer, P. von R.; Jiao, H. Aromaticity of Annelated Borepins. *Organometallics* **1997**, *16* (11), 2362–2369.

(95) Messersmith, R. E.; Siegler, M. A.; Tovar, J. D. Aromaticity Competition in Differentially Fused Borepin-Containing Polycyclic Aromatics. *J. Org. Chem.* **2016**, *81* (13), 5595–5605.

(96) Srivastava, A. K.; Misra, N. The Boron–Carbon–Nitrogen Heterocyclic Rings. *Chemical Physics Letters* **2015**, *625*, 5–9.

(97) Xu, S.; Mikulas, T. C.; Zakharov, L. N.; Dixon, D. A.; Liu, S.-Y. Boron-Substituted 1,3-Dihydro-1,3-Azaborines: Synthesis, Structure, and Evaluation of Aromaticity. *Angew. Chem., Int. Ed.* **2013**, *52* (29), 7527–7531.

(98) Chattaraj, P. K.; Roy, D. R. Aromaticity in Polyacene Analogues of Inorganic Ring Compounds. *J. Phys. Chem. A* **2007**, *111* (21), 4684–4696.

(99) Catão, A. J. L.; López-Castillo, A. Stability and Molecular Properties of the Boron-Nitrogen Alternating Analogs of Azulene and Naphthalene: A Computational Study. *J. Mol. Mod.* **2017**, *23* (4).

(100) Phukan, A. K.; Kalagi, R. P.; Gadre, S. R.; Jemmis, E. D. Structure, Reactivity and Aromaticity of Acenes and Their BN Analogues: A Density Functional and Electrostatic Investigation. *Inorg. Chem.* **2004**, *43* (19), 5824–5832.

(101) Barnard, J. H.; Brown, P. A.; Shuford, K. L.; Martin, C. D. 1,2-Phosphaborines: Hybrid Inorganic/Organic P–B Analogues of Benzene. *Angew. Chem., Int. Ed.* **2015**, *54* (41), 12083–12086.

(102) Nyulaszi, L. Aromaticity of Phosphorus Heterocycles. *Chem. Rev. (Washington, D. C.)* **2001**, *101* (5), 1229–1246.

(103) Lee, V. Y.; Sekiguchi, A. Aromaticity of Group 14 Organometallics: Experimental Aspects. *Angew. Chem., Int. Ed.* **2007**, *46* (35), 6596–6620.
(104) Goldfuss, B.; Schleyer, P. von R. Aromaticity in Group 14 Metalloles: Structural, Energetic, and Magnetic Criteria. *Organometallics* **1997**, *16* (8), 1543–1552.
(105) De Proft, F.; Fowler, P. W.; Havenith, R. W. A.; Schleyer, P. von R.; Van Lier, G.; Geerlings, P. Ring Currents as Probes of the Aromaticity of Inorganic Monocycles: P5−, As5−, S2N2, S3N3−, S4N3+, S4N42+, S5N5+, S42+ and Se42+. *Chemistry – A European Journal* **2004**, *10* (4), 940–950.
(106) Jimenez-Halla, J. O. C.; Matito, E.; Robles, J.; Sola, M. Nucleus-Independent Chemical Shift (NICS) Profiles in a Series of Monocyclic Planar Inorganic Compounds. *J. Organomet. Chem.* **2006**, *691* (21), 4359–4366.
(107) Maslowsky, E. Inorganic Metallocenes: The Structures and Aromaticity of Sandwich Compounds of the Transition Elements with Inorganic Rings. *Coordination Chemistry Reviews* **2011**, *255* (23), 2746–2763.
(108) Boldyrev, A. I.; Wang, L.-S. All-Metal Aromaticity and Antiaromaticity. *Chem. Rev. (Washington, DC, U. S.)* **2005**, *105* (10), 3716–3757.
(109) I. Boldyrev, A.; Wang, L.-S. Beyond Organic Chemistry: Aromaticity in Atomic Clusters. *Phys. Chem. Chem. Phys.* **2016**, *18* (17), 11589–11605.
(110) Tsipis, C. A. DFT Study of "All-Metal" Aromatic Compounds. *Coordination Chemistry Reviews* **2005**, *249* (24), 2740–2762.
(111) Khatua, S.; R. Roy, D.; Bultinck, P.; Bhattacharjee, M.; K. Chattaraj, P. Aromaticity in Cyclic Alkali Clusters. *Physical Chemistry Chemical Physics* **2008**, *10* (18), 2461–2474.
(112) Poater, J.; Sola, M.; Vinas, C.; Teixidor, F. Hueckel's Rule of Aromaticity Categorizes Aromatic Closo Boron Hydride Clusters. *Chem. - Eur. J.* **2016**, *22* (22), 7437–7443.
(113) Wannere, C. S.; Corminboeuf, C.; Wang, Z.-X.; Wodrich, M. D.; King, R. B.; Schleyer, P. v. R. Evidence for d Orbital Aromaticity in Square Planar Coinage Metal Clusters. *J. Am. Chem. Soc.* **2005**, *127* (15), 5701–5705.
(114) Tsipis, A. C.; Kefalidis, C. E.; Tsipis, C. A. The Role of the 5f Orbitals in Bonding, Aromaticity, and Reactivity of Planar Isocyclic and Heterocyclic Uranium Clusters. *J. Am. Chem. Soc.* **2008**, *130* (28), 9144–9155.
(115) Torres-Vega, J. J.; Vásquez-Espinal, A.; Caballero, J.; Valenzuela, M. L.; Alvarez-Thon, L.; Osorio, E.; Tiznado, W. Minimizing the Risk of Reporting False Aromaticity and Antiaromaticity in Inorganic Heterocycles Following Magnetic Criteria. *Inorg. Chem.* **2014**, *53* (7), 3579–3585.
(116) Báez-Grez, R.; Rabanal-León, W. A.; Alvarez-Thon, L.; Ruiz, L.; Tiznado, W.; Pino-Rios, R. Aromaticity in Heterocyclic Analogues of Benzene: Dissected NICS and Current Density Analysis. *J. Phys. Org. Chem.* **2019**, *32* (1), e3823.
(117) Foroutan-Nejad, C.; Vícha, J.; Ghosh, A. Relativity or Aromaticity? A First-Principles Perspective of Chemical Shifts in Osmabenzene and Osmapentalene Derivatives. *Phys. Chem. Chem. Phys.* **2020**.
(118) Badri, Z.; Pathak, S.; Fliegl, H.; Rashidi-Ranjbar, P.; Bast, R.; Marek, R.; Foroutan-Nejad, C.; Ruud, K. All-Metal Aromaticity: Revisiting the Ring Current Model among Transition Metal Clusters. *J. Chem. Theory Comput.* **2013**, *9* (11), 4789–4796.
(119) Seal, P. Is Nucleus-Independent Chemical Shift Scan a Reliable Aromaticity Index for Planar and Neutral A2B2 Clusters? *Journal of Molecular Structure: THEOCHEM* **2009**, *893* (1), 31–36.
(120) Foroutan-Nejad, C. Is NICS a Reliable Aromaticity Index for Transition Metal Clusters? *Theor Chem Acc* **2015**, *134* (2), 8.
(121) Schmidt, M. W.; Baldridge, K. K.; Boatz, J. A.; Elbert, S. T.; Gordon, M. S.; Jensen, J. H.; Koseki, S.; Matsunaga, N.; Nguyen, K. A.; Su, S.; Windus, T. L.; Dupuis, M.; Montgomery, J. A.

General Atomic and Molecular Electronic Structure System. *J. Comput. Chem.* **1993**, *14*, 1347–1363.

(122) Gordon, M. S.; Schmidt, M. W. Advances in Electronic Structure Theory: GAMESS a Decade Later. In *Theory and Applications of Computational Chemistry: the first forty years*; Elsevier, 2005; pp 1167–1189.

(123) te Velde, G.; Bickelhaupt, F. M.; Baerends, E. J.; Fonseca Guerra, C.; van Gisbergen, S. J. A.; Snijders, J. G.; Ziegler, T. Chemistry with ADF. *J. Comput. Chem.* **2001**, *22* (9), 931–967.

(124) Rahalkar, A. P.; Stanger, A. "Aroma", Http://Schulich.Technion.Ac.Il/Amnon_Stanger.Htm.

(125) Jug, K.; Koester, A. M. Aromaticity as a Multi-Dimensional Phenomenon. *J. Phys. Org. Chem.* **1991**, *4* (3), 163–169.

(126) Katritzky, A. R.; Karelson, M.; Sild, S.; Krygowski, T. M.; Jug, K. Aromaticity as a Quantitative Concept. 7. Aromaticity Reaffirmed as a Multidimensional Characteristic. *J. Org. Chem.* **1998**, *63* (15), 5228–5231.

(127) Fias, S.; Van Damme, S.; Bultinck, P. Multidimensionality of Delocalization Indices and Nucleus-Independent Chemical Shifts in Polycyclic Aromatic Hydrocarbons II: Proof of Further Nonlocality. *J. Comput. Chem.* **2010**, *31* (12), 2286–2293.

(128) Solà, M. Why Aromaticity Is a Suspicious Concept? Why? *Frontiers in Chemistry* **2017**, *5* (22).

(129) Balaban, A. T. Using Clar Sextets for Two- and Three-Dimensional Aromatic Systems. *Phys. Chem. Chem. Phys.* **2011**, *13* (46), 20649–20658.

(130) Portella, G.; Poater, J.; Sola, M. Assessment of Clar's Aromatic π-Sextet Rule by Means of PDI, NICS and HOMA Indicators of Local Aromaticity. *J. Phys. Org. Chem.* **2005**, *18* (8), 785–791.

(131) Ruiz-Morales, Y. The Agreement between Clar Structures and Nucleus-Independent Chemical Shift Values in Pericondensed Benzenoid Polycyclic Aromatic Hydrocarbons: An Application of the Y-Rule. *J. Phys. Chem. A* **2004**, *108* (49), 10873–10896.

(132) Gutman, I.; Ruiz-Morales, Y. Note on the Y-Rule in Clar Theory. *Polycyclic Aromatic Compounds* **2007**, *27* (1), 41–49.

(133) Oña-Ruales, J. O.; Ruiz-Morales, Y. Extended Y-Rule Method for the Characterization of the Aromatic Sextets in Cata-Condensed Polycyclic Aromatic Hydrocarbons. *J. Phys. Chem. A* **2014**, *118* (51), 12262–12273.

(134) Herndon, W. C.; Mills, N. S. Aromatic Stabilization Energy Calculations for the Antiaromatic Fluorenyl Cation. Issues in the Choice of Reference Systems for Positively Charged Species. *J. Org. Chem.* **2005**, *70* (21), 8492–8496.

(135) Mo, Y.; Schleyer, P. von R. An Energetic Measure of Aromaticity and Antiaromaticity Based on the Pauling-Wheland Resonance Energies. *Chem. - Eur. J.* **2006**, *12* (7), 2009–2020.

(136) Berionni, G.; Wu, J. I.-C.; Schleyer, P. v. R. Aromaticity Evaluations of Planar [6]Radialenes. *Org. Lett.* **2014**, *16* (23), 6116–6119.

(137) Kumar, C.; Fliegl, H.; Sundholm, D. Relation Between Ring Currents and Hydrogenation Enthalpies for Assessing the Degree of Aromaticity. *J. Phys. Chem. A* **2017**, *121* (38), 7282–7289.

(138) Mucsi, Z.; Viskolcz, B.; Csizmadia, I. G. A Quantitative Scale for the Degree of Aromaticity and Antiaromaticity: A Comparison of Theoretical and Experimental Enthalpies of Hydrogenation. *J. Phys. Chem. A* **2007**, *111* (6), 1123–1132.

(139) Shishkin, O. V.; Omelchenko, I. V.; Krasovska, M. V.; Zubatyuk, R. I.; Gorb, L.; Leszczynski, J. Aromaticity of Monosubstituted Derivatives of Benzene. The Application of out-of-Plane Ring Deformation Energy for a Quantitative Description of Aromaticity. *Journal of Molecular Structure* **2006**, *791* (1), 158–164.

(140) Lu, T.; Chen, F. Multiwfn: A Multifunctional Wavefunction Analyzer. *J. Comput. Chem.* **2012**, *33* (5), 580–592.

(141) Kruszewski, J.; Krygowski, T. M. Definition of Aromaticity Based on the Harmonic Oscillator Model. *Tetrahedron Lett.* **1972**, No. 36, 3839–3842.

(142) Dobrowolski, J. Cz. Three Queries about the HOMA Index. *ACS Omega* **2019**.
(143) Ghosh, D.; Periyasamy, G.; Pati, S. K. Density Functional Theoretical Investigation of the Aromatic Nature of BN Substituted Benzene and Four Ring Polyaromatic Hydrocarbons. *Phys. Chem. Chem. Phys.* **2011**, *13* (46), 20627–20636.
(144) Aihara, J. Effect of Bond-Length Alternation on the Aromaticity of Benzene. *Bull. Chem. Soc. Jpn.* **1990**, *63* (7), 1956–1960.
(145) Choi, C. H.; Kertesz, M. Bond Length Alternation and Aromaticity in Large Annulenes. *J. Chem. Phys.* **1998**, *108* (16), 6681–6688.
(146) Bredas, J. L. Relationship between Band Gap and Bond Length Alternation in Organic Conjugated Polymers. *J. Chem. Phys.* **//**, *82* (8), 3808–3811.
(147) Wannere, C. S.; Sattelmeyer, K. W.; Schaefer, H. F., III; Schleyer, P. von R. Aromaticity: The Alternating C-C Bond Length Structures of [14]-, [18]-, and [22]Annulene. *Angew. Chem., Int. Ed.* **2004**, *43* (32), 4200–4206.
(148) Haigh, C. W.; Mallion, R. B. Proton Magnetic Resonance of Nonplanar Condensed Benzenoid Hydrocarbons. II. Theory of Chemical Shifts. *Mol. Phys.* **1971**, *22* (6), 955–970.
(149) TURBOMOLE V7.0 2015, a Development of University of Karlsruhe and Forschungszentrum Karlsruhe GmbH, 1989-2007, TURBOMOLE GmbH, since 2007; Available from Http://Www.Turbomole.Com.
(150) V. Baryshnikov, G.; R. Valiev, R.; N. Karaush, N.; F. Minaev, B. Aromaticity of the Planar Hetero[8]Circulenes and Their Doubly Charged Ions: NICS and GIMIC Characterization. *Phys. Chem. Chem. Phys.* **2014**, *16* (29), 15367–15374.
(151) Baryshnikov, G. V.; Karaush, N. N.; Valiev, R. R.; Minaev, B. F. Aromaticity of the Completely Annelated Tetraphenylenes: NICS and GIMIC Characterization. *J Mol Model* **2015**, *21* (6), 136.
(152) Charistos, N. D.; Muñoz-Castro, A. Induced Magnetic Field of Fullerenes: Role of σ- and π-Contributions to Spherical Aromatic, Nonaromatic, and Antiaromatic Character in C_{60}^{q} (q = +10, 0, −6, −12), and Related Alkali-Metal Decorated Building Blocks, $Li_{12}C_{60}$ and $Na_{6}C_{60}$. *J. Phys. Chem. C* **2018**, *122* (17), 9688–9698.
(153) Orozco-Ic, M.; Barroso, J.; Charistos, N. D.; Muñoz-Castro, A.; Merino, G. Consequences of Curvature on Induced Magnetic Field: The Case of Helicenes. *Chem. - Eur. J.* **2020**, *26* (1), 326–330.
(154) Sebastiani, D. Current Densities and Nucleus-Independent Chemical Shift Maps from Reciprocal-Space Density Functional Perturbation Theory Calculations. *ChemPhysChem* **2006**, *7* (1), 164–175.
(155) Dauben, H. J.; Wilson, J. D.; Laity, J. L. Diamagnetic Susceptibility Exaltation in Hydrocarbons. *J. Am. Chem. Soc.* **1969**, *91* (8), 1991–1998.
(156) Dauben, H. J.; Wilson, J. D.; Laity, J. L. Diamagnetic Susceptibility Exaltation as a Criterion of Aromaticity. In *Organic Chemistry: A Series of Monographs*; Elsevier, 1971; Vol. 16, pp 167–206.
(157) Childs, R. F.; Pikulik, I. Diamagnetic Susceptibilities and Susceptibility Exaltations of Some 7-Substituted Cycloheptatrienes. *Can. J. Chem.* **1977**, *55* (2), 259–265.
(158) Matito, E.; Duran, M.; Solà, M. The Aromatic Fluctuation Index (FLU): A New Aromaticity Index Based on Electron Delocalization. *The Journal of Chemical Physics* **2005**, *122* (1), 014109.
(159) Aim2000. *Journal of Computational Chemistry* **2001**, *22* (5), 545–559.
(160) Keith, T. A. AIMAll. TK Gristmill Software, Overland Park KS, USA 2019.
(161) Huertas, O.; Poater, J.; Fuentes-Cabrera, M.; Orozco, M.; Solà, M.; Luque, F. J. Local Aromaticity in Natural Nucleobases and Their Size-Expanded Benzo-Fused Derivatives. *J. Phys. Chem. A* **2006**, *110* (44), 12249–12258.

(162) Solà, M.; Feixas, F.; Jiménez-Halla, J. O. C.; Matito, E.; Poater, J. A Critical Assessment of the Performance of Magnetic and Electronic Indices of Aromaticity. *Symmetry* **2010**, *2* (2), 1156–1179.
(163) Noury, S.; Krokodis, X.; Fuster, F.; Silvi, B. TopMod Package. 1997.
(164) Varetto, U. Molekel 5.4.
(165) Santos, J. C.; Andres, J.; Aizman, A.; Fuentealba, P. An Aromaticity Scale Based on the Topological Analysis of the Electron Localization Function Including σ and π Contributions. *J. Chem. Theory Comput.* **2005**, *1* (1), 83–86.
(166) Poater, J.; Duran, M.; Solà, M.; Silvi, B. Theoretical Evaluation of Electron Delocalization in Aromatic Molecules by Means of Atoms in Molecules (AIM) and Electron Localization Function (ELF) Topological Approaches. *Chem. Rev.* **2005**, *105* (10), 3911–3947.
(167) Allan, C. S. M.; Rzepa, H. S. Chiral Aromaticities. AIM and ELF Critical Point and NICS Magnetic Analyses of Möbius-Type Aromaticity and Homoaromaticity in Lemniscular Annulenes and Hexaphyrins. *J. Org. Chem.* **2008**, *73* (17), 6615–6622.
(168) Santos, P. F. and J. C. Electron Localization Function as a Measure of Electron Delocalization and Aromaticity http://www.eurekaselect.com/75380/article (accessed Jun 15, 2020).
(169) Zhao, Y.; Xie, Q.; Sun, T.; Wu, J.; Zhu, J. Predicting an Antiaromatic Benzene Ring in the Ground State Caused by Hyperconjugation. *Chem. - Asian J.* **2019**, *14* (23), 4309–4314.
(170) Giambiagi, M.; Segre de Giambiagi, M.; dos Santos Silva, C. D.; Paiva de Figueiredo, A. Multicenter Bond Indices as a Measure of Aromaticity. *Phys. Chem. Chem. Phys.* **2000**, *2* (15), 3381–3392.
(171) Bultinck, P.; Ponec, R.; Van Damme, S. Multicenter Bond Indices as a New Measure of Aromaticity in Polycyclic Aromatic Hydrocarbons. *J. Phys. Org. Chem.* **2005**, *18* (8), 706–718.
(172) Roy, D. R.; Bultinck, P.; Subramanian, V.; Chattaraj, P. K. Bonding, Reactivity and Aromaticity in the Light of the Multicenter Indices. *J. Mol. Struct.: THEOCHEM* **2008**, *854* (1), 35–39.
(173) Szczepanik, D. W.; Andrzejak, M.; Dyduch, K.; Zak, E.; Makowski, M.; Mazur, G.; Mrozek, J. A Uniform Approach to the Description of Multicenter Bonding. *Phys. Chem. Chem. Phys.* **2014**, *16* (38), 20514–20523.
(174) Cioslowski, J.; Matito, E.; Solà, M. Properties of Aromaticity Indices Based on the One-Electron Density Matrix. *J. Phys. Chem. A* **2007**, *111* (28), 6521–6525.
(175) Matito, E. An Electronic Aromaticity Index for Large Rings. *Phys. Chem. Chem. Phys.* **2016**, *18* (17), 11839–11846.
(176) W. Szczepanik, D.; Andrzejak, M.; Dominikowska, J.; Pawełek, B.; M. Krygowski, T.; Szatylowicz, H.; Solà, M. The Electron Density of Delocalized Bonds (EDDB) Applied for Quantifying Aromaticity. *Phys. Chem. Chem. Phys.* **2017**, *19* (42), 28970–28981.